German Research School
for Simulation Sciences

German Research School for Simulation Sciences

Combined Analysis of Lorentz- and Stieltjes-transformed Electromagnetic Response Functions of Light Nuclei

Master's Thesis

Nikhil Vaidya

October 13, 2015

Supervisor
Dr. Andreas Nogga

Examiner
Prof. Jörg Pretz

Co-Examiner
Prof. Ulf Meißner

Acknowledgements

I would like to thank my supervisor Dr. Andreas Nogga for his valuable guidance, innumerable explanations and suggestions. He was always available to answer my frequent questions and he has taught me a lot about scientific research in general. He also gave me the freedom to pursue my own ideas which motivated me considerably. My thanks to Dr. Susanna Liebig, Dr. Jan Bsaisou, Christopher Körber for their valuable suggestions.

I am especially grateful to my family and my parents. I thank them for their unconditional support and encouragement in all my activities.

Finally, I would like to thank my colleagues at the IKP for offering a friendly working atmosphere which made the whole experience thoroughly enjoyable.

Declaration

I hereby declare that I have written this thesis independently, and that I have not used any material apart from the declared sources.

Abstract

It is usual for observables related to inclusive electron scattering on light nuclei to be parametrised in terms of response functions. To calculate the response function, it is necessary to find the bound state of the nucleus, define the action of the so-called current operator, and to solve a scattering problem to find the final states of the nucleus. For a nucleus containing more than two nucleons, the scattering problem is especially difficult to solve because of the complex singularity structure of the relevant integral equations.

In the past, integral transformations have been used to calculate the response function. The integral transformations of the response function can be calculated using integral equations that no more possess any singularity. Unfortunately, the problem then lies in the inversion of the integral transform, since this is an ill-posed inverse problem and its solutions are numerically unstable.

In this thesis the goal is to investigate the effectiveness of using two different integral transforms (Stieltjes- and Lorentz-transforms) of the response functions as the output in the inverse problem.

Contents

List of Figures

List of Tables

1. Introduction

The strong interaction is still not very well understood and cannot be treated in perturbation theory. Binding energies are one way to study the strong interaction. Besides binding energies, external probes can be used to obtain information about the strong interaction. Probes that interact through weak or electromagnetic interactions can provide important information about the structure of nuclei or hadrons. The advantage of electromagnetically interacting probes is the large reaction cross-section and consequently, a greater amount of information. Yet, the electromagnetic interaction is weak enough to be treated in perturbation theory. The interaction between electrons and photons is very well understood. When it is expanded in perturbation theory, the electromagnetic interaction has terms scaled by powers of α ($\alpha \approx \frac{1}{137} \ll 1$), the fine structure constant. This means that a 1-photon exchange is a very good approximation because the higher order terms are very small in magnitude.

For the most simple case of elastic scattering, one can extract the form factors of the nucleus from the scattering data. This provides important information on, e.g. the charge distribution, the magnetic structure and many other properties of the nucleus. Even more detailed information can be obtained by studying break-up reactions where the nucleus disintegrates due to the electromagnetic interaction.

This thesis is concerned with ab-initio calculations of inclusive scattering cross-sections. Ab-initio calculations are the ones where the interaction hamiltonian and the kinematic conditions of the reaction are the only inputs, and all relevant degrees of freedom of the system are treated explicitly. In inclusive electron scattering, among all the particles obtained after the reaction, only the final momentum of the electron is measured. Theoretical calculations of the cross-section, therefore, require a summation over all the final states of the nuclear system. It will be shown in Section 2.2 that the inclusive scattering cross section is completely characterised by two response functions. It involves a summation over all final states of the nucleons and depends only of the photon energy and three momentum. A naive calculation of the response function would require dealing with continuum states of nuclei with asymptotic boundary conditions [2]. This is very difficult to do even for a small number of particles. An extension of the Lippman-Schwinger equations to the three body case has already been carried out through the Faddeev-Yakubowsky equations ([4] and [18]). The application of these equations to exclusive electron scattering on ^{3}He are in [6] and [10]. Yet, this approach is still very difficult for systems consisting of four or more nucleons.

A way around this difficulty is the calculation of integral transforms of the response functions from bound state matrix elements [1]. This is followed by an inversion of the integral transform to obtain the response function. The integral transforms can be computed using bound state techniques as we shall see below. Bound state techniques remove the difficulty of dealing with continuum states with complicated asymptotic boundary conditions or singularities of corresponding integral equations. The motivation behind this idea is, for the cross section, the complete scattering wave function is not required and some of the information in the scattering state can be left out [2].

The choice of the kernel of the integral transformation is important. The reason for this is the need of inversion of the integral transform. The inversion of the integral transform is generally an ill-posed problem. This means that small errors in the integral transform can be magnified by the method used to solve the inverse problem. The Stieltjes kernel has already been used in [1] and [3]. The results obtained from this method are not satisfactory. The Lorentz transformation method has been used to calculate inclusive scattering response functions of ^{3}He and ^{3}H in [12]. The problem with this approach is that, in some cases, it gives response functions with unphysical oscillations or those which are not positive in the complete range of ω. The idea in this thesis is to use both transforms for the purpose of the inversion, with the hope that the different information in the Stieltjes and Lorentz transform will together help calculate response functions with a smaller error.

In this thesis, I use both the Stieltjes and Lorentz-transforms to calculate inclusive electron-scattering response functions for the deuteron. In Chapter 2 I will derive an expression for the cross-section of electron-deuteron inclusive scattering and show explicitly the dependence on the longitudinal and transverse response functions. This requires modelling the interaction between the electron and the nucleus. I fix the S-Matrix up to second order in the electromagnetic interaction. I also assume that two nucleon currents can be ignored. This means that the photon interacts with the nucleons as if the nucleons were free particles. I will use the non-relativistic approximation for the nuclear part of the currents which is justified for the energy range considered. This is derived in Section 2.3.

Section 3.1 contains the partial-wave decomposition of the nuclear current operator. Throughout this thesis, I will work in momentum space. The section first introduces the momentum space basis used for all dynamical equations and to represent the deuteron bound state wave function. Then in Section 3.2 I show, starting from the definitions of the Stieltjes- and Lorentz-transforms of the response function, that the integral transforms can be determined only using bound state techniques. The integral transforms can be determined as matrix elements of quantum states that solve an inhomogeneous Schrödinger-like equation. This inhomogeneous equation involves no singularities and is therefore similar to a bound state problem. With the help of this non-homogeneous equation, given the deuteron wave-function, one can calculate the Stieltjes- and Lorentz-transforms of the inclusive electron-scattering response functions.

The next step is to back-transform the response functions from their integral transforms. Since the problem of back-transformation is ill-posed, it is highly sensitive to errors in

the integral transform. There exists the issue of error magnification.The methods used to perform the back-transformation are discussed in Chapter 4. There are parameters in these back transformation methods whose values need to be fixed. One more important aspect of this chapter is the determination of these parameters with a priori knowledge of the correct back-transformation result. Furthermore, Section 4.2 contains a description of the back-transformation techniques used in this thesis. In Section 4.3 the back-transformation methods are used to find the response function for a test case and their stability with respect to the number of energy grid points is discussed. For the test case, analytical expressions are available and this helps us to directly compare the quality of the back-transformed response function to the exact one. Separated analyses are carried out using the Stieltjes- and Lorentz-transforms and their results are compared to those obtained when both integral transforms are combined. I stress here that The back transformations used are not based on special basis sets that might introduce a bias towards a special functional form of the result.

In Chapter 5 I apply the back-transformation methods to find response functions using realistic potentials. For the realistic potentials the back transformations are performed using the method of Tikhonov Regularization (TR) [16]. This method is described in detail in Section 4.2. One of the important aspects of this chapter is the determination of the optimum back-transformation parameters without a priori knowledge of the correct back transformation results. The methodology used to find the optimum parameters of this method for the realistic potentials is performed in Chapter 5. This chapter also contains the results of the calculated deuteron response functions and discussions about their quality.

Finally, Chapter 6 contains the conclusion and outlook.

2. Formalism

In this chapter I present the derivation of the cross-section for inclusive electron scattering on a two nucleon system. In inclusive electron scattering, only the outgoing electron is detected and hence, we need to sum over all final states of the two nucleon system. It will be shown that the cross-section depends on two response functions. That will be followed by the derivation of the non-relativistic approximation of the cross-section.

2.1. Scattering Cross-section and the S-Matrix

In the reference frame where the target is at rest, the cross-section of a reaction is defined in [14] as

$$d\sigma = \frac{\text{Number of Events/Time}}{\text{Number of target particles} \cdot \text{Flux of projectile particles}} \tag{2.1}$$

The probability amplitude of measuring a final state $\big|f\big\rangle$ after the interaction, given the initial state was $\big|i\big\rangle$, is defined as the S-matrix element

$$S_{fi} = \big\langle f\big|S\big|i\big\rangle \tag{2.2}$$

The probability of measuring a final state in an infinitesimal neighbourhood of dN_f (density of final states) around $\big|f\big\rangle$, is therefore

$$p = |S_{fi}|^2 \cdot dN_f \tag{2.3}$$

For this calculation one examines a target and a projectile in a volume V and a measuring time T. In the rest-frame of the target, the projectile has a velocity v_P

$$d\sigma = \frac{|S_{fi}|^2 \cdot dN_f/(T \cdot V)}{\frac{1}{V} \cdot v_p V} \tag{2.4}$$

I fix the S-Matrix up to the second order in the electromagnetic interaction. Also, since the effect of the two nucleon currents is small, they will be ignored in this thesis. I therefore

assume that the photon interacts with the deuteron via a 1-nucleon current. The interaction Hamiltonian density can be written as

$$\begin{aligned}\mathcal{H}_I(x) &=: j_N^\mu(x)\cdot A_\mu(x) + j_e^\mu(x)\cdot A_\mu(x) :\\ \text{where } j_e^\mu(x) &= e_e\bar{\psi}\cdot\gamma^\mu\cdot\psi_e(x)\\ \text{and } j_N^\mu(x) &= e_P\int d^4y d^4y'\bar{\psi(y)}\cdot\Gamma^\mu(y,y',x)\cdot\psi(y').\end{aligned} \tag{2.5}$$

where j_N^μ is given in momentum space in equation (67) of [7]. ψ_e, $\bar{\psi}_e$ and ψ, $\bar{\psi}$ are the field operators of the electron and nucleons respectively. I distinguish the protons and neutrons through their isospin, and therefore their field operators possess eight components. I, therefore, get for the S-Matrix,

$$\begin{aligned}\langle f|S|i\rangle &= \langle f|Texp(-i\int d^4x\mathcal{H}_I(x))|i\rangle\\ &= \frac{(-i)^2}{2!}\langle f|T\int d^4x_1\int d^4x_2\mathcal{H}(x_1)\mathcal{H}(x_2)|i\rangle\\ &= (-i)^2\int d^4x_1\int d^4x_2\langle f|Tj_e^\mu(x_1)\cdot A_\mu(x_1)j_N^\nu(x_2)\cdot A_\nu(x_2)|i\rangle.\end{aligned} \tag{2.6}$$

The initial and final states each contain one electron and two nucleons. With the help of Wick's theorem, I can contract the field operators of the photons to obtain

$$\langle f|S|i\rangle \;=\; (-i)^2\int d^4x_1\int d^4x_2\langle ks|j_e^\mu(x_1)|k's'\rangle\langle\Psi P|j_N^\nu(x_2)|\Psi' P'\rangle\overbrace{A_\mu(x_1)A_\nu}(x_2). \tag{2.7}$$

Here, the deuteron initial and final states $|\Psi' P'\rangle$ and $|\Psi P\rangle$ have third components of total angular momentum m_i and m_f respectively. The contraction of the photon fields is given by

$$\overbrace{A_\mu(x_1)A_\nu}(x_2) = i\int\frac{d^4Q}{(2\pi)^4}\frac{e^{-iQ(x_1-x_2)}}{Q^2+i\epsilon}(-ig_{\mu\nu}). \tag{2.8}$$

which is the photon propagator. The momentum and spin for an incoming and outgoing electron are k', s' and k, s respectively. The initial and final states of the two nucleon system posses the total four momenta P' and P respectively. The translation of the current operators gives

$$\begin{aligned}j_e^\mu &= e^{i\hat{P}x_1}j_e^\mu(0)e^{-i\hat{P}x_1}\\ j_N^\mu &= e^{i\hat{P}x_2}j_N^\mu(0)e^{-i\hat{P}x_2}.\end{aligned} \tag{2.9}$$

Since the incoming and outgoing states are eigenstates of the momentum operator, I can replace the momentum operator $\hat{P}$ with the respective eigenvalues. I can, therefore, easily substitute the translated currents of equation (2.9) in equation (2.7). The x-integrations

produce two δ-functions and the S-Matrix element simplifies to

$$\begin{aligned}\langle f|S|i\rangle &= (-i)^2 \int d^4x_1 \int d^4x_2 \int \frac{d^4Q}{(2\pi)^4} \frac{-1 g_{\mu\nu}}{Q^2+i\epsilon} e^{iQ(x_1-x_2)} \langle ks|j_e^\mu(0)|k's'\rangle \langle \Psi P|j_N^\nu|\Psi' P'\rangle \\ & e^{i(k-k')x_1} e^{i(P-P')x_2} \\ &= (2\pi)^4 \delta^4(k-k'+P-P') \frac{1}{Q^2+i\epsilon} \langle ks|j_e^\mu(0)|k's'\rangle \langle \Psi P|j_N^\nu(0)|\Psi' P'\rangle \\ &\text{with } Q = k'-k = P-P' = (\omega, \vec{Q}). \end{aligned} \tag{2.10}$$

To calculate the cross-section, the S-Matrix element needs to be squared. For this purpose I use

$$\delta^4(0) = \int \frac{d^x}{(2\pi)^4} e^{-i0\cdot x} = \frac{1}{(2\pi)^4} \int d^4x = \frac{V\cdot T}{(2\pi)^4} \tag{2.11}$$

as given in [11] on page 139. I have computed the integral over the finite physical system with volume V and a measuring time T. The result will no longer depend on these quantities. I then substitute the S-Matrix into the definition (2.4) of the reaction cross-section and obtain

$$\begin{aligned} d\sigma &= (2\pi)^4 \delta^4(k-k'+P-P') \frac{1}{Q^2+i\epsilon} \cdot \frac{1}{Q^2-i\epsilon} \cdot VT \frac{e_e^2 e_p^2}{V^4} \frac{m^2}{k_0 k_0'} \frac{MM'}{P_0 P_0'} V^2 \frac{1}{VT} \frac{1}{|v_{k'}|} \\ &\Big| \underbrace{\langle ks| \sqrt{\frac{k_0 k_0'}{m^2}} \frac{V}{e_e} j_e^\mu(0)|k's'\rangle}_{L^\mu} \underbrace{\langle \Psi P| \sqrt{\frac{P_0 P_0'}{MM'}} \frac{V}{e_p} j_\mu^N(0)|\Psi' P'\rangle}_{N_\mu} \Big|^2 dN_f \\ &= (2\pi)^4 \delta^4(k+P-k'-P') \frac{1}{Q^4+i\epsilon} \cdot \frac{1}{Q^4-i\epsilon} \frac{e^4}{V^2} \frac{m^2}{k_0 k_0'} \frac{MM'}{P_0 P_0'} \frac{k_0'}{|\vec{k'}|} L_\mu L_\nu^* N^\mu N^{\mu *} dN_f \end{aligned} \tag{2.12}$$

, where m is the rest mass of the electron. The number of states dN_f after the interaction is given in terms of the outgoing momenta d^3k, d^3P and the inner degrees of freedom df as

$$dN_f = \frac{V}{(2\pi)^3} d^3k \frac{V}{(2\pi)^3} d^3P \cdot df. \tag{2.13}$$

M and M' are the rest masses of the final and initial states of the deuteron with ${P_0'}^2 = {M'}^2 + {\vec{P'}}^2$ and $P_0^2 = M^2 + \vec{P}^2$. For inclusive scattering, a summation must be carried out over all final states of the deuteron, but the final state of the electron is fixed.

$$d\sigma = \int df \int d^3P' \frac{1}{(2\pi)^2} \delta^4(k+P-k'-P') \frac{e^4}{Q^4+i\epsilon} L_\mu L_\nu^* N^\mu N^{\nu *} \frac{k_0'}{|\vec{k'}|} \frac{m^2}{k_0 k_0'} \frac{MM'}{P_0 P_0'} k^2 d\hat{k} dk \tag{2.14}$$

In the rest frame of the target, we have $P' = (M', \vec{0})$. In the following part I assume that the electrons are highly relativistic. Therefore, I can neglect their rest masses compared to

their momenta.

$$\begin{aligned} k'_0 &= |\vec{k'}| \\ k_0 &= |\vec{k}| \quad dk_0 = dk \end{aligned} \tag{2.15}$$

With this approximation we have from equation (2.14)

$$\begin{aligned} \frac{d\sigma}{d\hat{k}d\hat{k_0}} &= \frac{m^2}{(2\pi)^2}\int df \int d^3P\delta^4(k+P-k'-P')\frac{e^4}{Q^4+i\epsilon}\frac{k_0}{k'_0}\frac{M}{P_0}L_\mu L^*_\nu N^\mu N^{\nu *} \\ &= \frac{m^2}{(2\pi)^2}\frac{k_0}{k'_0}\int df\delta(k_0-k'_0+P_0-M')\frac{e^4}{Q^4}\frac{M}{P_0}L_\mu L^*_\nu N^\mu N^{\nu *}. \end{aligned} \tag{2.16}$$

In the last step I used the three-momentum relation to carry out the integration. Through this step, $\vec{P} = \vec{k'} - \vec{k} \equiv \vec{Q}$ is established.

Finally a sum over the final spins m_f and s and an average over the initial spins m_i and s' remains. Since the electron has spin $\frac{1}{2}$ and and the deuteron has a spin 1, there are two additional factors of $\frac{1}{2}$ and $\frac{1}{3}$.

$$\frac{d\sigma}{d\hat{k}dk_0} = \frac{m^2}{(2\pi)^2}\frac{k_0}{k'_0}\int df\delta(k_0-k'_0+P'_0-M)\frac{e^4}{Q^4}\frac{M}{P_0}\frac{1}{2}\sum_{ss'}L_\mu L^*_\nu\frac{1}{3}\sum_{m_f m_i}N^\mu N^{\nu *} \tag{2.17}$$

In the following section I will derive the averaging of spins for the electronic matrix element L_μ and define two response functions that will contain the nuclear matrix elements N_μ.

2.2. Spin Averaging and Response Functions

The electronic matrix element L_μ simplifies as

$$\begin{aligned} L^\mu &= \langle ks|\sqrt{\frac{k_0k'_0}{m^2}}\frac{V}{e_e}j^\mu_e(0)|k's'\rangle \\ &= V\sqrt{\frac{k_0k'_0}{m^2}}\langle ks|\bar{\psi}_e(0)\gamma_\mu\psi_e(0)|k's'\rangle \\ &= \sqrt{k_0k'_0}\sum\!\!\!\!\!\!\int_l \frac{d^3p}{\sqrt{p_0}}\sum\!\!\!\!\!\!\int_{l'}\frac{d^3p'}{\sqrt{p'_0}}\langle ks|\mathrm{b}^\dagger(p'l')\mathrm{b}(pl)|k's'\rangle\bar{u}(p'l')\gamma^\mu u(pl) \\ &\qquad \text{for } |k's'\rangle \neq |ks\rangle \\ &= \bar{u}(ks)\gamma^\mu u(k's') \end{aligned} \tag{2.18}$$

For the calculation, I have used the standard commutation relations of the creation and annihilation operators b, $\mathrm{b}^\dagger$, d and $\mathrm{d}^\dagger$. I substitute the expression for the electronic matrix

element in the summation of equation (2.17) and obtain

$$\begin{aligned}
\frac{1}{2}\sum_{ss'} L_\mu L_\nu^* &= \frac{1}{2}\sum_{ss'} \bar{u}(ks)\gamma^\mu u(k's')[\bar{u}(ks)\gamma_\nu u(k's')]^* \\
&= \frac{1}{2}\sum_{ss'} \bar{u}(ks)\gamma^\mu u(k's')u^\dagger(k's')\gamma_\nu^\dagger\gamma_0 u(ks) \\
&= \frac{1}{2}\sum_{ss'} \bar{u}(ks)\gamma^\mu \bar{u}(k's')\underbrace{\gamma_0\gamma_\nu^\dagger\gamma_0}_{\gamma_\nu} u(k's') \\
&= \frac{1}{2}\sum_{ss'} \mathrm{Tr}(\gamma_\mu u(k's')\bar{u}(k's')\gamma_\nu u(ks)\bar{u}(ks)) \\
&= \frac{1}{2}\sum_{ss'} \mathrm{Tr}\left(\gamma_\mu \frac{\not{k}'+m}{2m}\gamma_\nu \frac{\not{k}+m}{2m}\right) \\
&= \frac{1}{8m^2}\cdot 4\cdot(k'_\mu k_\nu + k_\mu k'_\nu - k'\cdot k g_{\mu\nu} + m^2 g_{\mu\nu}) \\
&= \frac{1}{2m^2}\left(\frac{1}{2}(k+k')_\mu(k'+k)_\nu - \frac{1}{2}\underbrace{(k'-k)_\mu}_{Q_\mu}\underbrace{(k'-k)_\nu}_{Q_\nu} + \frac{1}{2}g_{\mu\nu}Q^2\right).
\end{aligned} \tag{2.19}$$

In the fourth step I have used the following completeness relation of the u-Spinors:

$$\sum_s u(ks)\bar{u}(ks) = \frac{\not{k}+m}{2m} \tag{2.20}$$

and evaluated the trace using,

$$\{\gamma^\mu,\gamma^\nu\} = 2g^{\mu\nu}. \tag{2.21}$$

Using current conservation, the nuclear part simplifies as

$$\begin{aligned}
\partial_\mu\langle\varphi P|j_N^\mu(x)|\varphi' P'\rangle = \partial_\mu e^{i(P'-P)x}\langle\varphi P|j_N^\mu(0)|\varphi' P'\rangle &= 0 \\
(P-P')_\mu\langle\varphi P|j_N^\mu(0)|\varphi' P'\rangle &= 0 \\
Q_\mu N^\mu &= 0.
\end{aligned} \tag{2.22}$$

Since $L_\mu L_\nu^*$ and $N^\mu N^{\nu *}$ will be multiplied, I shall substitute

$$\sum_{ss'} L_\mu L_\nu^* = \frac{1}{2m^2}\big(\frac{1}{2}(k+k')_\mu(k+k')_\nu + \frac{1}{2}g_\mu\nu Q^2\big). \tag{2.23}$$

From now on I use a special coordinate system in which $\vec{Q} = (0,0,Q_z)$ and $\vec{K} := (\vec{k}+\vec{k'}) = (K_x,0,K_z)$. The relation $\partial_\mu j_N^\mu(x) = 0$ ensures that not all nuclear matrix elements are

independent of each other.

$$\begin{aligned} Q_\mu N^\mu &= Q_0 N^0 - Q_z N_z = 0 \\ \Rightarrow \qquad N_z &= \frac{Q_0}{Q_z} N^0 = \frac{Q_0}{|\vec{Q}|} N^0 \end{aligned} \tag{2.24}$$

For practical reasons, in the following calculation, I make use of spherical components.

$$\begin{aligned} \hat{e}_1 &= -\frac{1}{\sqrt{2}}(\hat{e}_x + i\hat{e}_y) \\ \hat{e}_{-1} &= \frac{1}{\sqrt{2}}(\hat{e}_x - i\hat{e}_y) \\ \hat{e}_0 &= \hat{e}_z \end{aligned} \tag{2.25}$$

The spherical components of $\vec{N}$ are given by

$$\begin{aligned} \vec{N} &= N_1 \hat{e}_1^* + N_{-1}\hat{e}_{-1}^* + \frac{Q_0}{|\vec{Q}|} N^0 \hat{e}_0^* \\ \text{with } N_1 &= \vec{N} \cdot \hat{e}_1 = -\frac{1}{\sqrt{2}}(N_x + iN_y) \\ N_{-1} &= \vec{N} \cdot \hat{e}_1 = \frac{1}{\sqrt{2}}(N_x - iN_y). \end{aligned} \tag{2.26}$$

The scalar products are evaluated using the co-ordinate system and the spherical components given above.

$$\begin{aligned} K \cdot N &= (k + k')_\mu N^\mu = (K_0 - K_z \frac{Q_0}{|\vec{Q}|}) N^0 + \frac{1}{\sqrt{2}} K_x (N_1 - N_{-1}) \\ N \cdot N^* &= \left(1 - \frac{Q_0^2}{|\vec{Q}|^2}\right) |N^0|^2 - (|N_1|^2 + |N_{-1}|^2) \\ &= -\frac{Q^2}{|\vec{Q}|^2} |N^0|^2 - (|N_1|^2 + |N_{-1}|^2) \end{aligned} \tag{2.27}$$

Substituting that and equation (2.23) in the reaction cross-section leads to

$$\begin{aligned}
\frac{d\sigma}{d\hat{k}dk_0} &= \frac{m^2}{(2\pi)^2}\frac{k_0}{k_0'}\int df \frac{e^4}{Q^4}\frac{M}{P_0}\frac{1}{2J+1}\sum_{m_i m_f} N^\mu N^{\nu *}\frac{1}{2m^2} \\
&\quad \left(\frac{1}{2}K_\mu K_\nu + \frac{1}{2}g_{\mu\nu}Q^2\right)\cdot\delta(k_0 - k_0' + P_0 - M') \\
&= \frac{1}{4}\frac{1}{(2\pi)^2}\frac{k_0}{k_0'}\frac{e^4}{Q^4}\int df \frac{M}{P_0}\frac{1}{3}\sum_{m_i m_f}\Bigg[\left(K_0 - K_z\frac{Q_0}{|\vec{Q}|}\right)^2|N_0|^2 \\
&\quad + \frac{1}{2}K_x^2(|N_1|^2 + |N_{-1}|^2 - N_1N_{-1}^* - N_1^*N_{-1}) + \frac{1}{\sqrt{2}}\left(K_0 - K_z\frac{Q_0}{|\vec{Q}|}\right) \\
&\quad K_x(N_0N_1^* - N_0N_{-1}^* + N_0^*N_1 - N_0^*N_{-1}) \\
&\quad - \left(\frac{Q^4}{|\vec{Q}|^2}|N_0|^2 + Q^2(|N_1|^2 + |N_{-1}|^2)\right)\Bigg]\delta(\underbrace{k_0 - k_0'}_{-\omega} + P_0 - M'). \qquad (2.28)
\end{aligned}$$

The spin sums over the interference terms $N_0N_{-1}^*$, $N_0N_1^*$ etc. are zero, because the products disappear for a target that has been polarised in the $\hat{Q}$ direction. For unpolarised targets, one can choose the direction of quantisation to be $\hat{Q}$. This causes the interference terms to disappear and the reaction cross-section simplifies to

$$\begin{aligned}
\frac{d\sigma}{d\hat{k}dk_0} &= \frac{1}{4}\frac{1}{(2\pi)^2}\frac{k_0}{k_0'}\frac{e^4}{Q^4}\int df \frac{M}{P_0}\frac{1}{3}\sum_{m_i m_f}\delta(-\omega + P_0 - M') \\
&\quad \Bigg[\left(K_0 - K_z\frac{Q_0}{|\vec{Q}|}\right)^2|N_0|^2 - \frac{Q^4}{|\vec{Q}|^2}|N_0|^2 \\
&\quad + \left(\frac{1}{2}K_x^2 - Q^2\right)(|N_1|^2 - |N_{-1}|^2)\Bigg]. \qquad (2.29)
\end{aligned}$$

For the calculation of kinematic factors in front of $|N_0|^2$ and $|N_1|^2 + |N_{-1}|^2$ one uses again the approximation that the electrons are highly relativistic, with $k_0 \approx |\vec{k}|$.

$$\begin{aligned}
\left(K_0 - K_z\frac{Q_0}{|\vec{Q}|}\right)^2 - \frac{Q^4}{|\vec{Q}|^2} &= \left((k_0 + k_0') - (\vec{k'} + \vec{k})\cdot\frac{(\vec{k'} - \vec{k})}{|\vec{Q}|}\frac{Q_0}{|\vec{Q}|}\right) - \frac{Q^4}{|\vec{Q}|^2} \\
&= \left((k_0 + k_0') - (k_0 + k_0')\frac{(k_0' - k_0)}{|\vec{Q}|}\frac{Q_0}{|\vec{Q}|}\right) - \frac{Q^4}{|\vec{Q}|^2} \\
&= (k_0 + k_0')^2\left(1 - \frac{Q_0^2}{|\vec{Q}|^2}\right)^2 - \frac{Q^4}{|\vec{Q}|^2} \\
&= \frac{Q^4}{|\vec{Q}|^4}\left[(k_0 + k_0')^2 - (\vec{k'} - \vec{k})^2\right] \\
&= \frac{Q^4}{|\vec{Q}|^4} 2k_0k_0'(1 + \cos\theta) \\
&= \frac{Q^4}{|\vec{Q}|^4} 4k_0k_0'\cos^2\frac{\theta}{2}
\end{aligned} \tag{2.30}$$

where θ is the angle between the incoming and outgoing momenta $\vec{k'}$ and $\vec{k}$ respectively of the electron. The second term is obtained using the same approximation as

$$\begin{aligned}
\frac{1}{2}K_x^2 - Q^2 &= \frac{1}{2}(|\vec{K}|^2) - K_z^2) - Q^2 \\
&= \frac{1}{2}\left((\vec{k} - \vec{K'})^2 - ((\vec{k} + \vec{k'})\cdot(\vec{k'} - \vec{k}))^2\frac{1}{|\vec{Q}|^2}\right) - Q^2 \\
&= \frac{1}{2|\vec{Q}|^2}((\vec{k} + \vec{k'})^2(\vec{k'} - \vec{k})^2 - ((\vec{k} + \vec{k'})\cdot(\vec{k'} - \vec{k}))^2) - Q^2 \\
&= \frac{2}{|\vec{Q}|^2}k_0^2k_0'(1 - \cos^2\theta) - Q^2.
\end{aligned} \tag{2.31}$$

With Q^2 given as

$$\begin{aligned}
Q^2 &= (k_0' - k_0)^2 - (\vec{k'} - \vec{k})^2 \\
&= -2k_0k_0'(1 - \cos\theta) = -4k_0k_0'\sin^2\frac{\theta}{2}.
\end{aligned} \tag{2.32}$$

It follows that

$$\begin{aligned}
\frac{1}{2}K_x^2 - Q^2 &= \frac{8}{|\vec{Q}|^2}k_0^2k_0'^2\cos^2\frac{\theta}{2}\sin^2\frac{\theta}{2} + 4k_0k_0'\sin^2\frac{\theta}{2} \\
&= 4k_0k_0'\cos^2\frac{\theta}{2}\left[-\frac{Q^2}{2|\vec{Q}|^2} + \tan^2\frac{\theta}{2}\right].
\end{aligned} \tag{2.33}$$

The substitution of these expressions in the cross-section in equation (2.29) gives

$$\frac{d\sigma}{d\hat{k}dk_0} = \overbrace{\frac{1}{4}\frac{1}{(2\pi)^2}\frac{k_0}{k_0'}\frac{e^4}{Q^4}4k_0k_0'\cos^2\frac{\theta}{2}}^{\sigma_{Mott}} \left[\underbrace{\frac{Q^4}{|\vec{Q}|^4}}_{v_L}\underbrace{\int df\frac{1}{2J+1}\sum_{m_im_f}\delta(-\omega+P_0'-M)\frac{M'}{P_0'}|N_0|^2}_{R_L} + \underbrace{\left[-\frac{Q^2}{2|\vec{Q}|^2}+\tan^2\frac{\theta}{2}\right]}_{v_T} \underbrace{\int df\frac{1}{3}\sum_{m_im_f}\delta(-\omega+P_0'-M)\frac{M'}{P_0'}(|N_1|^2+|N_{-1}|^2)}_{R_T}\right]. \tag{2.34}$$

I have separated the Mott reaction cross-section σ_{Mott} for the scattering of two spin-$\frac{1}{2}$ particles without internal structure. The change in the cross-section due to the structure of the nucleon systems is essentially contained in two response functions, the longitudinal $R_L(\omega, |\vec{Q}|)$ and the transversal $R_T(\omega, |\vec{Q}|)$. For the calculation of the response functions I need to look into the action of the nuclear current operators. From the experimental data, both functions can be determined individually.

2.3. Non-relativistic Approximation of the Nuclear Matrix Element

In this thesis the nuclear matrix element shall be derived in a non-relativistic approximation. This approximation is justified because the momenta of the deuteron are small compared to the mass of the nucleons. Apart from this, the energy transfer is not so large as to create

further hadrons (e.g mesons). The initial and final states of the deuteron are therefore,

$$\begin{aligned}
\big|\Psi P\big\rangle &= \sum\!\!\!\!\!\!\int_{m_1 t_1} d^3p_1 \sum\!\!\!\!\!\!\int_{m_2 t_2} d^3p_2 \Psi(\vec{p_1} m_1 t_1, \vec{p_2} m_2 t_2) \\
&\quad \cdot \frac{1}{\sqrt{2!}} \mathrm{b}^\dagger(\vec{p_2} m_2 t_2) \mathrm{b}^\dagger(\vec{p_1} m_1 t_1) \big|0\big\rangle \\
&\equiv \sum\!\!\!\!\!\!\int_{m_1 t_1} d^3p_1 \sum\!\!\!\!\!\!\int_{m_2 t_2} d^3p_2 \Psi(\vec{p_1}\vec{p_2}) \frac{1}{\sqrt{2!}} \mathrm{b}_2^\dagger \mathrm{b}_1^\dagger \big|0\big\rangle \\
\big|\Psi' P'\big\rangle &= \sum\!\!\!\!\!\!\int_{m_1' t_1'} d^3p_1' \sum\!\!\!\!\!\!\int_{m_2' t_2'} d^3p_2' \Psi'(\vec{p_1'}\vec{p_2'}) \frac{1}{\sqrt{2!}} \mathrm{b}_{2'}^\dagger \mathrm{b}_{1'}^\dagger \big|0\big\rangle \\
&\qquad (\big|0\big\rangle \text{is the vacuum state})
\end{aligned} \tag{2.35}$$

where, Ψ and Ψ' are the antisymmetric wave functions of the initial and final states of the two nucleons. To make the following derivation short, I will group under the name $\vec{p_i}$ all degrees of freedom of the i^{th} nucleon, namely $\vec{p_i}$ m_i t_i. m_i and t_i are the third components of the spin and isospin of the nucleons respectively. The wave functions Ψ and Ψ' also fix the centre of mass momenta P and P' respectively.

$$\begin{aligned}
\Psi(\vec{p_1}\vec{p_2}) &= \tilde{\Psi}(\vec{p_1}\vec{p_2}) \delta(\vec{p_1} + \vec{p_2} - \vec{P}) \\
\Psi'(\vec{p_1'}\vec{p_2'}) &= \tilde{\Psi}'(\vec{p_1'}\vec{p_2'}) \delta(\vec{p_1'} + \vec{p_2'} - \vec{P'})
\end{aligned} \tag{2.36}$$

Given the centre of mass momentum and a single particle momentum, the second particle momentum can be determined. I therefore use the Jacobi co-ordinates. The relative momentum between particles 1 and 2 is given by,

$$\vec{p} = \frac{1}{2}(\vec{p_1} - \vec{p_2}) \tag{2.37}$$

I can now derive the nuclear matrix elements

$$\begin{aligned}
N_\mu &= \big\langle \Psi' P' \big| V \frac{P_0 P_0'}{M M'} \frac{1}{e_P} j_\mu^N(0) \big| \Psi P \big\rangle \\
&= \sum\!\!\!\!\!\!\int_{m_1 t_1 m_2 t_2} d^3p_1 d^3p_2 \sum\!\!\!\!\!\!\int_{m_1' t_1' m_2' t_2'} d^3p_1' d^3p_2' \\
&\quad \frac{1}{2!} \Psi'^*(\vec{p_1'}\vec{p_2'}) \Psi(\vec{p_1}\vec{p_2}) \\
&\quad \big\langle 0 \big| \mathrm{b}_{1'} \mathrm{b}_{2'} \frac{1}{e_P} j_\mu^N(0) \mathrm{b}_2^\dagger \mathrm{b}_1^\dagger \big| 0 \big\rangle \cdot V \sqrt{\frac{P_0 P_0'}{M M'}}
\end{aligned} \tag{2.38}$$

I use the expression for $j_\mu^N(0)$ from [7] (equation number 67) and obtain

$$\begin{aligned} N_\mu = & \sum\!\!\!\!\!\!\int_{m_1 t_1 m_2 t_2} d^3p_1 d^3p_2 \sum\!\!\!\!\!\!\int_{m_1' t_1' m_2' t_2'} d^3p_1' d^3p_2' \\ & \frac{1}{2!}\Psi'^*(\vec{p_1'}\vec{p_2'})\Psi(\vec{p_1}\vec{p_2}) \\ & \sum\!\!\!\!\!\!\int_{m_p t_p} d^3p \sum\!\!\!\!\!\!\int_{m_p' t_p'} d^3p' \frac{1}{V}\sqrt{\frac{m_N^2}{p_0 p_0'}}\bar{u}(\vec{p})\mathcal{F}_\mu((\vec{p}-\vec{p'})^2)u(\vec{p'}) \\ & \left\langle 0\middle|\mathrm{b}_{1'}\mathrm{b}_{2'}\mathrm{b}_p^\dagger\mathrm{b}_{p'}\mathrm{b}_2^\dagger\mathrm{b}_1^\dagger\middle|0\right\rangle \cdot V\sqrt{\frac{P_0 P_0'}{MM'}}. \end{aligned} \tag{2.39}$$

where I use the shorthand

$$\begin{aligned} \mathcal{F}_\mu((\vec{p}-\vec{p'})^2) = & \Pi_p(F_1^p((\vec{p}-\vec{p'})^2)\gamma_\mu + i\sigma_{\mu\nu}(p-p')^\nu F_2^p((\vec{p}-\vec{p'})^2)) \\ & + \Pi_n(F_1^n((\vec{p}-\vec{p'})^2)\gamma_\mu + i\sigma_{\mu\nu}(p-p')^\nu F_2^n((\vec{p}-\vec{p'})^2)). \end{aligned} \tag{2.40}$$

Here Π_p and Π_n are so called isospin projection operators. They project any isospin state onto a proton and neutron isospin state respectively. F_1 and F_2 are the Dirac and Pauli nucleon form factors respectively [7]. I will evaluate the matrix element $\left\langle 0\middle|\mathrm{b}_{1'}\mathrm{b}_{2'}\mathrm{b}_p^\dagger\mathrm{b}_{p'}\mathrm{b}_2^\dagger\mathrm{b}_1^\dagger\middle|0\right\rangle$ in which I will exchange the positions of the creation and annihilation operators till an annihilation operator acts on a vacuum state. The following anti-commutator relation is used.

$$\{\mathrm{b}^\dagger(\vec{p_i}m_i t_i), \mathrm{b}^\dagger(\vec{p_j}m_j t_j)\} = \delta_{m_i m_j}\delta_{t_i t_j}\delta(\vec{p_i}-\vec{p_j}) \equiv \delta_{ij} \tag{2.41}$$

The matrix element is given by

$$\begin{aligned} \left\langle 0\middle|\mathrm{b}_{1'}\mathrm{b}_{2'}\mathrm{b}_p^\dagger\mathrm{b}_{p'}\mathrm{b}_2^\dagger\mathrm{b}_1^\dagger\middle|0\right\rangle = & \delta_{p2'}(\delta_{2p'}\delta_{11'} - \delta_{21'}\delta_{1p'}) \\ & - \delta_{1'p}(\delta_{2p'}\delta_{12'} - \delta_{2'2}\delta_{p1}). \end{aligned} \tag{2.42}$$

By renaming integration and summation variables and using the antisymmetry of the wave functions, one finds out that all 4 terms is equation (2.42) give the same result. We therefore

obtain

$$\begin{aligned} N_\mu = 4 \cdot & \sum\!\!\!\!\!\!\int_{m_1 t_1 m_2 t_2} d^3p_1 d^3p_2 \sum\!\!\!\!\!\!\int_{m_1' t_1' m_2' t_2'} d^3p_1' d^3p_2' \sum\!\!\!\!\!\!\int_{m_p t_p} d^3p \sum\!\!\!\!\!\!\int_{m_p' t_p'} d^3p' \\ & \frac{1}{2}\sqrt{\frac{P_0 P_0'}{MM'}\frac{m_N^2}{p_0 p_0'}}\bar{u}(\vec{p})\mathcal{F}_\mu((\vec{p}-\vec{p'})^2)u(\vec{p'}) \\ & \delta_{1'p}\delta_{1p'}\delta_{22'}\Psi'^*(\vec{p'}_1\vec{p'}_2)\Psi(\vec{p}_1\vec{p}_2) \\ = 2 \cdot & \sum\!\!\!\!\!\!\int_{m_1' t_1'} d^3p_1' \sum\!\!\!\!\!\!\int_{m_1 t_1 m_2 t_2} d^3p_1 d^3p_2 \sqrt{\frac{P_0 P_0'}{MM'}\frac{m_N^2}{p_0 p_0'}} \\ & \bar{u}(\vec{p_1'})\mathcal{F}_\mu((\vec{p_1'}-\vec{p_1})^2)u(\vec{p_1})\Psi'^*(\vec{p_1'}\vec{p_2})\Psi(\vec{p_1}\vec{p_2}). \end{aligned} \tag{2.43}$$

Now using equations (2.36) and (2.37) I get

$$\begin{aligned} N_\mu = 2 \cdot & \sum\!\!\!\!\!\!\int_{m_1' t_1'} d^3p_1' \sum\!\!\!\!\!\!\int_{m_1 t_1 m_2 t_2} d^3p_1 d^3p_2 \sqrt{\frac{P_0 P_0'}{MM'}\frac{m_N^2}{p_0 p_0'}} \\ & \bar{u}(\vec{p_1'})\mathcal{F}_\mu((\vec{p_1'}-\vec{p_1})^2)u(\vec{p_1})\tilde{\Psi}'^*(\vec{p_1'}\vec{p_2})\tilde{\Psi}(\vec{p_1}\vec{p_2})\delta(\vec{p}_1+\vec{p}_2-\vec{P})\delta(\vec{p'}_1+\vec{p}_2-\vec{P'}). \end{aligned} \tag{2.44}$$

I first change the momenta p_1 and p_2 to Jacobi momenta p and P. The determinant of the Jacobian is 1 for this change of variables. The delta functions are used to remove the integrals over p_1' and P. Additionally, I make use of the momentum relation

$$\vec{p'} = \vec{p} + \frac{1}{2}(\vec{P'} - \vec{P}) = \frac{1}{2}\vec{Q} + \vec{p}. \tag{2.45}$$

This leads to

$$\begin{aligned} N_\mu = 2 \cdot & \sum\!\!\!\!\!\!\int_{m_1' t_1'} d^3p \sum_{m_1 t_1 m_2 t_2} \sqrt{\frac{P_0 P_0'}{MM'}\frac{m_N^2}{p_0 p_0'}} \\ & \bar{u}(\vec{Q}+\vec{p})\mathcal{F}_\mu(\vec{Q}^2)u(\vec{p})\tilde{\Psi}'^*(\vec{p}+\frac{\vec{Q}}{2})\tilde{\Psi}(\vec{p}). \end{aligned} \tag{2.46}$$

In the non-relativistic limit we have $\sqrt{\frac{P_0 P_0'}{MM'}\frac{m_N^2}{p_0 p_0'}} \approx 1$. We also have

$$\begin{aligned}\bar{u}(\vec{p_1'})\mathcal{F}_\mu(\vec{Q}^2)u(\vec{p_1}) &= \bar{u}(\vec{p_1'}m_1't_1')(\Pi_p(F_1^p(\vec{Q}^2)\gamma_\mu + i\sigma_{\mu\nu}Q^\nu F_2^p(\vec{Q}^2))) \\ &\quad (\Pi_n(F_1^n(\vec{Q}^2)\gamma_\mu + i\sigma_{\mu\nu}Q^\nu F_2^n(\vec{Q}^2)))u(\vec{p_1}m_1t_1) \\ &= \delta_{t_1\frac{1}{2}}\delta_{t_1t_1'}(F_1^p(\vec{Q}^2)\bar{u}(\vec{p_1}'m_1')\gamma_\mu u_p(\vec{p_1}m_1) + iF_2^p(\vec{Q}^2)Q^\nu \bar{u}_p(\vec{p_1}'m_1')\sigma_{\mu\nu}u_p(\vec{p_1}m_1)) \\ &+ \delta_{t_1,-\frac{1}{2}}\delta_{t_1t_1'}(F_1^n(\vec{Q}^2)\bar{u}_n(\vec{p_1}'m_1')\gamma_\mu u_n(\vec{p_1}m_1) + iF_2^n(\vec{Q}^2)Q^\nu \bar{u}_n(\vec{p_1}'m_1')\sigma_{\mu\nu}u_n(\vec{p_1}m_1)).\end{aligned} \tag{2.47}$$

Using the Dirac representation of spinors, with a non-relativistic approximation, and the Gordon-decomposition from [13] I get, for $\mu = 0$,

$$\begin{aligned}\bar{u}_p(\vec{p'}_1m_1')\gamma_0 u_p(\vec{p}_1m_1) &= \bar{u}_n(\vec{p'}_1m_1')\gamma_0 u_n(\vec{p}_1m_1) \\ &= \underbrace{\sqrt{\frac{p_1^{0\prime}+m_N}{2m_N}}}_{\approx 1}\underbrace{\sqrt{\frac{p_1^0+m_N}{2m_N}}}_{\approx 1}\begin{bmatrix}\chi_{m_1'} \\ \frac{\vec{\sigma}\cdot\vec{p'}_1}{p_1^{0\prime}+m_N}\chi_{m_1'}\end{bmatrix}^\dagger\begin{bmatrix}\chi_{m_1} \\ \frac{\vec{\sigma}\cdot\vec{p}_1}{p_1^0+m_N}\chi_{m_1}\end{bmatrix} \\ &\approx \chi^\dagger_{m_1'}\chi_{m_1} + \underbrace{\frac{p_1'^i p_1^j}{(p_1^{0\prime}+m_N)(p_1^0+m_N)}}_{\approx 0}\chi^\dagger_{m_1'}\sigma_i^\dagger\sigma_k\chi_{m_1} \\ &\approx \delta_{m_1m_1'}.\end{aligned} \tag{2.48}$$

I read off only the spin operator part and obtain

$$= 1. \tag{2.49}$$

For $\mu \neq 0$ the expression is slightly more complicated,

$$\begin{aligned}
\bar{u}_p(\vec{p'}_1 m'_1)\gamma_\mu u_p(\vec{p}_1 m_1) &= \bar{u}_n(\vec{p'}_1 m'_1)\gamma_\mu u_n(\vec{p}_1 m_1) \\
&= \underbrace{\sqrt{\frac{p_1^{0\prime}+m_N}{2m_N}}}_{\approx 1}\underbrace{\sqrt{\frac{p_1^0+m_N}{2m_N}}}_{\approx 1}\begin{bmatrix}\chi_{m'_1}\\ \frac{\vec{\sigma}\cdot\vec{p'}_1}{p_1^{0\prime}+m_N}\chi_{m'_1}\end{bmatrix}^\dagger\begin{bmatrix}0 & \sigma_\mu\\ \sigma_\mu & 0\end{bmatrix}\begin{bmatrix}\chi_{m_1}\\ \frac{\vec{\sigma}\cdot\vec{p}_1}{p_1^0+m_N}\chi_{m_1}\end{bmatrix} \\
&\approx \chi^\dagger_{m'_1}\sigma_\mu\underbrace{\frac{\vec{\sigma}\cdot\vec{p}_1}{p_1^0+m_N}}_{\approx 2m_N}\chi_{m_1} + \chi^\dagger_{m'_1}\underbrace{\frac{\vec{\sigma}^\dagger\cdot\vec{p'}_1}{p_1^{\prime 0}+m_N}}_{\approx 2m_N}\sigma_\mu\chi_{m_1} \\
&\approx \chi^\dagger_{m'_1}\sigma_\mu\frac{\sigma_i p_1^i}{2m_N}\chi_{m_1} + \chi^\dagger_{m'_1}\frac{\sigma_j p_1^{\prime j}}{2m_N}\sigma_\mu\chi_{m_1} \\
&= \frac{\chi^\dagger_{m'_1}\chi_{m_1}}{2m_N}(\delta_{\mu i}p_1^i + \delta_{\mu j}p_1^{\prime j}) + \frac{ip_1^i\epsilon_{\mu ic}\chi^\dagger_{m'_1}\sigma_c\chi_{m_1}}{2m_N} + \frac{ip_1^{\prime j}\epsilon_{j\mu c}\chi^\dagger_{m'_1}\sigma_c\chi_{m_1}}{2m_N} \\
&= \frac{\delta_{m_1,m'_1}}{2m_N}(p_1^\mu + p_1^{\prime\mu}) - \frac{i(p_1^{\prime i}-p_1^i)\epsilon_{\mu ic}\chi^\dagger_{m'_1}\sigma_c\chi_{m_1}}{2m_N} \\
&= \frac{\delta_{m_1,m'_1}}{2m_N}(p_1^\mu + p_1^{\prime\mu}) - \frac{i(Q^i)\epsilon_{\mu ic}\chi^\dagger_{m'_1}\sigma_c\chi_{m_1}}{2m_N} \\
&= \frac{\delta_{m_1,m'_1}}{2m_N}(p_1^\mu + p_1^{\prime\mu}) - \frac{i\chi^\dagger_{m'_1}(\vec{Q}\times\vec{\sigma})^\mu\chi_{m_1}}{2m_N}.
\end{aligned} \tag{2.50}$$

In the second term, I read off only the spin operator part and obtain

$$= \frac{1}{2m_N}(p_1^\mu + p_1^{\prime\mu}) + i\frac{(\vec{\sigma}\times\vec{Q})^\mu}{2m_N}. \tag{2.51}$$

Now I look separately at three cases depending on μ and ν. I will derive the expressions for $\bar{u}_p(\vec{p'}_1 m'_1)\sigma^{\mu\nu}u_p(\vec{p}_1 m_1)$ and $\bar{u}_n(\vec{p'}_1 m'_1)\sigma^{\mu\nu}u_n(\vec{p}_1 m_1)$. We have, for the first case $\mu = 0$

($\nu = 0$ does not contribute)

$$\begin{aligned}
\bar{u}_p(\vec{p'}_1 m'_1)\sigma^{\mu\nu}u_p(\vec{p}_1 m_1) &= \bar{u}_n(\vec{p'}_1 m'_1)\sigma^{\mu\nu}u_n(\vec{p}_1 m_1) \\
&= i\underbrace{\sqrt{\frac{p_1^{0\prime}+m_N}{2m_N}\frac{p_1^0+m_N}{2m_N}}}_{\approx 1}\begin{bmatrix}\chi_{m'_1}\\ \frac{\vec{\sigma}\cdot\vec{p'_1}}{p_1^{0\prime}+m_N}\chi_{m'_1}\end{bmatrix}^\dagger\begin{bmatrix}1 & 0\\ 0 & -1\end{bmatrix}\begin{bmatrix}0 & \sigma^\nu\\ \sigma^\nu & 0\end{bmatrix}\begin{bmatrix}\chi_{m_1}\\ \frac{\vec{\sigma}\cdot\vec{p_1}}{p_1^0+m_N}\chi_{m_1}\end{bmatrix} \\
&\approx i\begin{bmatrix}\chi_{m'_1}\\ \frac{\vec{\sigma}\cdot\vec{p'_1}}{p_1^{0\prime}+m_N}\chi_{m'_1}\end{bmatrix}^\dagger\begin{bmatrix}0 & \sigma^\nu\\ -\sigma^\nu & 0\end{bmatrix}\begin{bmatrix}\chi_{m_1}\\ \frac{\vec{\sigma}\cdot\vec{p_1}}{p_1^0+m_N}\chi_{m_1}\end{bmatrix} \\
&= i\left[-\underbrace{\frac{p_1^{\prime i}}{p_1^{\prime 0}+m_N}}_{\approx 0}\chi^\dagger_{m'_1}\sigma^{i\dagger}\sigma^\nu\chi_{m_1} + \underbrace{\frac{p_1^j}{p_1^0+m_N}}_{\approx 0}\chi^\dagger_{m'_1}\sigma^\nu\sigma^j\chi_{m_1}\right] \approx 0.
\end{aligned} \tag{2.52}$$

In the second case $\mu \neq 0$ and $\nu = 0$, using the same arguments for the non-relativistic limit, we get

$$\begin{aligned}
\bar{u}_p(\vec{p'}_1 m'_1)\sigma^{\mu\nu}u_p(\vec{p}_1 m_1) &= \bar{u}_n(\vec{p'}_1 m'_1)\sigma^{\mu\nu}u_n(\vec{p}_1 m_1) \\
&\approx 0
\end{aligned} \tag{2.53}$$

since, the Q^0 term from equation (2.47) is negligible in the non-relativistic limit. Finally for the third case $\mu \neq 0$ and $\nu \neq 0$, I re-label μ and ν as i and j. Then using the approximations for the non-relativistic limit, we get

$$\begin{aligned}
\bar{u}_p(\vec{p'}_1 m'_1)\sigma^{ij}u_p(\vec{p}_1 m_1) &= \bar{u}_n(\vec{p'}_1 m'_1)\sigma^{ij}u_n(\vec{p}_1 m_1) \\
&\approx \frac{i}{2}\begin{bmatrix}\chi_{m'_1}\\ \frac{\vec{\sigma}\cdot\vec{p'_1}}{p_1^{0\prime}+m_N}\chi_{m'_1}\end{bmatrix}^\dagger\begin{bmatrix}1 & 0\\ 0 & -1\end{bmatrix}\begin{bmatrix}[\sigma^j,\sigma^i] & 0\\ 0 & [\sigma^j,\sigma^i]\end{bmatrix}\begin{bmatrix}\chi_{m_1}\\ \frac{\vec{\sigma}\cdot\vec{p_1}}{p_1^0+m_N}\chi_{m_1}\end{bmatrix} \\
&\approx \frac{i}{2}\cdot 2i\begin{bmatrix}\chi_{m'_1}\\ \frac{\vec{\sigma}\cdot\vec{p'_1}}{p_1^{0\prime}+m_N}\chi_{m'_1}\end{bmatrix}^\dagger\begin{bmatrix}1 & 0\\ 0 & -1\end{bmatrix}\begin{bmatrix}\epsilon_{jik}\sigma^k & 0\\ 0 & \epsilon_{jik}\sigma^k\end{bmatrix}\begin{bmatrix}\chi_{m_1}\\ \frac{\vec{\sigma}\cdot\vec{p_1}}{p_1^0+m_N}\chi_{m_1}\end{bmatrix} \\
&\approx \epsilon_{ijk}\chi^\dagger_{m'_1}\sigma^k\chi_{m_1}.
\end{aligned} \tag{2.54}$$

Here I read off only the spin operator part for use in the further derivation.

$$\Rightarrow \epsilon_{ijk}\sigma^k \tag{2.55}$$

From the above derivations I read off the current operator as,

$$\Theta_\mu(\vec{Q}) = \begin{cases} \Pi_p F_1^p(\vec{Q}^2) + \Pi_n F_1^n(\vec{Q}^2) & \text{for } \mu = 0 \\ \Pi_p \big[\frac{p_1^{'\mu} + p_1^\mu}{2m_N} F_1^p(\vec{Q}^2) + i(\vec{\sigma} \times \vec{Q})^\mu (\frac{F_1^p(\vec{Q}^2)}{2m_N} + F_2^p(\vec{Q}^2))\big] & \\ + \Pi_n \big[\frac{p_1^{'\mu} + p_1^\mu}{2m_N} F_1^n(\vec{Q}^2) + i(\vec{\sigma} \times \vec{Q})^\mu (\frac{F_1^n(\vec{Q}^2)}{2m_N} + F_2^n(\vec{Q}^2))\big] & \text{for } \mu \neq 0 \end{cases} \tag{2.56}$$

The non-relativistic approximation for the nuclear matrix element is therefore obtained as

$$\begin{aligned} N_\mu &\approx 2 \cdot \sum\!\!\!\!\!\!\int_{m_1' m_1 t_1 m_2 t_2} d^3p \big\langle \tilde{\Psi}' \big| \vec{p} m_1' t_1 m_2 t_2 \big\rangle \big\langle \vec{p} m_1' t_1 m_2 t_2 \big| \Theta_\mu^1(\vec{Q}) \big| \vec{p} - \frac{\vec{Q}}{2} m_1 t_1 m_2 t_2 \big\rangle \big\langle \vec{p} - \frac{\vec{Q}}{2} m_1 t_1 m_2 t_2 \big| \Psi \big\rangle \\ &= 2 \cdot \big\langle \Psi' \big| \Theta_\mu^1(\vec{Q}) \big| \Psi \big\rangle. \end{aligned} \tag{2.57}$$

In equation (2.57), the current operator acts on particle 1. Since the states $\big|\varphi\big\rangle$ and $\big|\varphi'\big\rangle$ are antisymmetric under particle exchange, the following holds (The superscript of Θ_μ indicates the particle it is acting upon).

$$\big\langle \Psi' \big| \Theta_\mu^1(\vec{Q}) \big| \Psi \big\rangle = \big\langle \Psi' \big| \Theta_\mu^2(\vec{Q}) \big| \Psi \big\rangle \tag{2.58}$$

I can finally substitute the non-relativistic approximation of the nuclear matrix element in equation (2.34) and use the approximations $\frac{M'}{P_0'} \approx 1$ and $P_0' \approx M' + \frac{\vec{Q}^2}{2M}$ obtain the non-relativistic approximation to the response function.

$$R_L(\omega, |\vec{Q}|) = \frac{4}{3} \sum_{m_i m_f} \int df \delta(-\omega + \frac{\vec{Q}}{2M} + M' - M) |\big\langle \Psi_f m_f \big| \Theta_0(\vec{Q}) |\Psi_i m_i\big\rangle|^2 \tag{2.59}$$

$$\begin{aligned} R_T(\omega, |\vec{Q}|) = \frac{4}{3} \sum_{m_i m_f} \int df \delta(-\omega + \frac{\vec{Q}}{2M} + M' - M) \big(&|\big\langle \Psi_f m_f \big| \Theta_1(\vec{Q}) |\Psi_i m_i\big\rangle|^2 \\ &+ |\big\langle \Psi_f m_f \big| \Theta_{-1}(\vec{Q}) |\Psi_i m_i\big\rangle|^2 \big) \end{aligned} \tag{2.60}$$

All further derivations make use of this non-relativistic approximation.

3. Numerical Implementation

The most difficult aspect of the response function calculation is the implementation of the current operator of equation (2.56). I will describe the implementation of these operators in detail in this chapter. As mentioned in the introduction, I will use bound state techniques to calculate integral transforms of the response function.

3.1. Implementation of the Electromagnetic Current Operator

To calculate bound state matrix elements of the current operator from equation (2.56), we need to derive the partial wave decomposition of this operator in a two particle basis. What I focus on in this thesis are 1-body currents, since they have the most important contributions to the cross-section. I worked with the non-relativistic approximation of the one body current and its form as in [7] is given by

$$\langle \vec{p}|j^0(\vec{q})|\vec{p'}\rangle = \delta^3(\vec{p}-\vec{p'}-\vec{q}) \tag{3.1}$$

$$\langle \vec{p}|\vec{j}(\vec{q})|\vec{p'}\rangle = \left[\frac{1}{2m_N}(\vec{p}+\vec{p'}) + \frac{i}{2m_N}\vec{\sigma}\times\vec{q}\right]\delta^3(\vec{p}-\vec{p'}-\vec{q}). \tag{3.2}$$

The operator in (3.1) is called the longitudinal current and is a scalar operator, whereas the one in (3.2) is a vector operator and called the transverse current. The first part of the right hand side of equation (3.2) is called the convection current and the second one is called spin current. The $\vec{\sigma}$ is the spin operator for spin-1/2 particles. Since this is a 1-body current acting on a nucleon, it will be acting on either a neutron or a proton. The action of the 1-body current on the neutron and proton is different. This is not apparent from the way I have written equations (3.1) and (3.2), and this information will be contained in the isospin projection operators which I shall treat separately in another section.

To describe the effect of an electron scattering on a deuteron which is at rest in the lab frame, we need to calculate the matrix element $\langle p(ls)jm_jtm_t|j_\mu^{(1)}(\vec{q})\otimes\left(\Pi_n^{(1)}+\Pi_p^{(1)}\right)+j_\mu^{(2)}(\vec{q})\otimes\left(\Pi_n^{(2)}+\Pi_p^{(2)}\right)|\Psi,\vec{0}\rangle$. The number in the superscript indicates which particles is being acted upon. It will suffice to only derive the matrix element for the case when the operator acts on particle 1 and multiply the result by 2. This because of the Pauli principle and hence all states are antisymmetric in particles 1 & 2. The operators $\Pi_{p/n}$ are isospin projection

operators for the neutron and proton respectively. Note that this factor of 2 already appears in equation (2.57).

Longitudinal Current Operator

The longitudinal current operator drives the longitudinal response function. The action of the 1-body longitudinal current operator on a single particle momentum eigenstate is given by

$$\langle \vec{p}|j^0(\vec{q})|\vec{p'}\rangle = \delta^3(\vec{p} - \vec{p'} - \vec{q}). \tag{3.3}$$

To derive the action of the longitudinal current on the deuteron, I use the basis $|p(ls)jm_jtm_t\vec{P}\rangle$. In this basis, p is the magnitude of the relative momentum of the two nucleons in the deuteron. The vector $\vec{P}$ is the center of mass momentum of the deuteron. I define these two momenta as follows:

$$\begin{aligned} \vec{p} &= \frac{1}{2}(\vec{k_1} - \vec{k_2}) \\ \vec{P} &= \vec{k_1} + \vec{k_2} \end{aligned} \tag{3.4}$$

where $\vec{k_1}$ and $\vec{k_2}$ are the momenta of the two nucleons. The quantum number l is the total orbital angular momentum quantum number of the 2-nucleon system and s is the total spin quantum number. The notation $(ls)jm_j$ means that the quantum numbers l and s are coupled to give the total 2-nucleon angular momentum quantum number j with component m_j in the z-direction. The quantum numbers t and m_t are the total isospin and the z-component isospin of the 2-nucleon system. We are interested in finding an expression for the matrix element $\langle p(ls)jm_jtm_t|j_0^{(1)}(\vec{q})\otimes\Pi_{p/n}^{(1)}|p'(l's')j'm_j't'm_t'\rangle$. From the definition of the basis states we get

$$\begin{aligned} \langle p(ls)jm_jtm_t\vec{P}|j_0^{(1)}(\vec{q})\otimes\Pi_{p/n}^{(1)}|p'(l's')j'm_j't'm_t'\vec{P}'\rangle = \langle tm_t|\Pi_{p/n}^{(1)}|t'm_t'\rangle \cdot \\ \langle p(ls)jm_j\vec{P}|j_0^{(1)}(\vec{q})|p'(l's')j'm_j'\vec{P}'\rangle. \end{aligned} \tag{3.5}$$

I write the isospin matrix element $\langle tm_t|\Pi_{p/n}^{(1)}|t'm_t'\rangle$ as I in the remaining part of the derivation. This matrix element is derived in detail in equation (3.40).

I use the basis $|p(ls)jm_jtm_t\vec{P}\rangle$ because the deuteron wave function is available in this basis. Given that the current operator acts on single particle momentum eigenstates, I need to change from the basis mentioned earlier to the basis $|\vec{k_1}\vec{k_2}sm_stm_t\rangle$, where $\vec{k_1}$ and $\vec{k_2}$ are the momenta of the two nucleons and s and m_s are their combined spin quantum number and z-component of spin, respectively. As before, t and m_t are the total isospin quantum number and its z-component, respectively. To change from one basis to another, we insert the unit operator in the form of a complete set of states. For example, to change from the basis $|p(ls)jm_jtm_t\vec{P}\rangle$ to the basis $|\vec{k_1}\vec{k_2}sm_stm_t\rangle$, we insert the unit operator in the following

way:

$$\big|p(ls)jm_jtm_t\vec{P}\big\rangle = \sum\!\!\!\!\!\!\int_{m_s=-s}^{+s} d^3k_1 d^3k_2 \big|\vec{k_1}\vec{k_2}sm_stm_t\big\rangle\big\langle\vec{k_1}\vec{k_2}sm_stm_t\big|p(ls)jm_jtm_t\vec{P}\big\rangle. \quad (3.6)$$

To simplify the expression on the right hand side of equation (3.6) we need to evaluate the overlaps between two different kinds of basis states. Overlaps that I used frequently are given in appendix B. After suitable basis changes, equation (3.5) becomes,

$$= I \cdot \sum\!\!\!\!\!\!\int_{m_lm_l'm_s} d^3p_1 d^3p_2 (lsj, m_lm_sm_j)(l's'j', m_l'm_sm_j') \frac{\delta(p-p_1)}{p\cdot p_1}\frac{\delta(p'-p_2)}{p'\cdot p_2}\delta_{ss'}$$
$$Y^*_{lm_l}(\widehat{p_1})Y_{l'm_l'}(\widehat{p_2})\delta^3\left(\frac{\vec{P}+2\vec{p_1}}{2}-\frac{\vec{P'}+2\vec{p_2}}{2}-\vec{q}\right)\delta^3\left(\frac{\vec{P}-2\vec{p_1}}{2}-\frac{\vec{P'}-2\vec{p_2}}{2}\right). \quad (3.7)$$

Here, I have changed to a basis $\big|\vec{p}\vec{P}sm_stm_t\big\rangle$ (relative momentum vector and center of mass momentum vector)and $\widehat{p}$ represents the angular part of $\vec{p}$. The coefficients $(lsj, m_lm_sm_j)$ and $(l's'j', m_l'm_sm_j')$ are Clebsch-Gordan coefficients. They are overlaps between basis states of the type $\big\langle(ls)jm_j\big|lm_lsm_s\big\rangle$. They help to uncouple two coupled quantum numbers. $Y^*_{lm_l}(\widehat{p_1})$ and $Y_{l'm_l'}(\widehat{p_2})$ are spherical harmonics. They take as arguments, the angular parts of the relative momentum vectors of the out-going and in-coming states, respectively. I will use the result of equation (3.7) to calculate the matrix element we are interested in. This matrix element involves the action of the current operator on the deuteron bound state. For the calculation of the cross section, I work in the rest-frame of the deuteron, therefore in the following derivation, the deuteron momentum will be zero. Furthermore, since there is no restriction on the centre of mass momentum of the system after the interaction, I integrate over all final center of mass momenta. Hence the matrix element involving the action of the current operator on the deuteron bound state becomes

$$\int d^3P\big\langle p(ls)jm_jtm_tP\big|j_0^{(1)}(\vec{q})\otimes\Pi^{(1)}_{p/n}\big|\Psi\vec{0}\big\rangle = \sum\!\!\!\!\!\!\int_{\alpha'=\{l',s',j',t',m_t',m_j'\}} d^3P\cdot p'^2dp'\varphi_{\alpha'}(p')$$
$$\big\langle p(ls)jm_jtm_t\vec{P}\big|j_0^{(1)}(\vec{q})\cdot\Pi^{(1)}_{p/n}\big|p'(l's')j'm_j't'm_t'\vec{0}\big\rangle. \quad (3.8)$$

Where, $\big|\Psi\vec{0}\big\rangle$ is the deuteron bound state with the centre of mass at rest and $\varphi_{\alpha'}(p') = \big\langle p'\alpha'\big|\Psi\big\rangle$. Using the previous result, I get

$$= \sum\!\!\!\!\!\!\int_{\alpha'=\{l',s',j',t',m_t',m_j'\}} d^3P\cdot p'^2dp' I\cdot\varphi_{\alpha'}(p') \sum\!\!\!\!\!\!\int_{m_lm_l'm_s} d^3p_1d^3p_2(lsj,m_lm_sm_j)(l's'j',m_l'm_sm_j')$$
$$\frac{\delta(p-p_1)}{p\cdot p_1}\frac{\delta(p'-p_2)}{p'\cdot p_2}\delta_{ss'}Y^*_{lm_l}(\widehat{p_1})Y_{l'm_l'}(\widehat{p_2})\delta^3\left(\frac{\vec{P}+2\vec{p_1}}{2}-\vec{p_2}-\vec{q}\right)\delta^3\left(\frac{\vec{P}-2\vec{p_1}}{2}+\vec{p_2}\right). \quad (3.9)$$

In the above equation, the expressions inside the three-dimensional delta functions simplify as compared to equation (3.7) since $\vec{P}' = \vec{0}$. The above equation simplifies further by eliminating summations over some quantum numbers by using the property of Clebsch-Gordan coefficients that $(lsj, m_l m_s m_j) \propto \delta_{m_j, m_l + m_s}$. Two more simplifications are possible by eliminating the integrals $\int d^3P$, $\int p'^2 dp'$ and d^3p_2 using the delta functions $\delta^3\left(\frac{\vec{P}-2\vec{p_1}}{2} + \vec{p_2}\right)$, $\frac{\delta(p'-p_2)}{p' \cdot p_2}$ and $\delta^3\left(\frac{\vec{P}+2\vec{p_1}}{2} - \vec{p_2} - \vec{q}\right)$ respectively.

$$= \sum\!\!\!\!\!\!\int_{\alpha'=\{l',s,j',t',m_t',m_j'\}} I \sum\!\!\!\!\!\!\int_{m_l m_l' m_s} d^3p_1 (lsj, m_l m_s m_j)(l'sj', m_l' m_s m_j') \varphi_{\alpha'}\left(\left|\vec{p_1} - \frac{1}{2}\vec{q}\right|\right) \frac{\delta(p-p_1)}{p \cdot p_1} Y^*_{lm_l}(\hat{p_1}) Y_{l'm_l'}(\widehat{\vec{p_1} - \frac{1}{2}\vec{q}}) \quad (3.10)$$

In the next step I split the remaining integral $\int d^3p_1$ into magnitude and angular parts. I further eliminate the integral over the magnitude with the help of the delta function $\frac{\delta(p-p_1)}{p \cdot p_1}$. I therefore obtain

$$= \sum\!\!\!\!\!\!\int_{\alpha'=\{l',s,j',t',m_t',m_j'\}} I \sum\!\!\!\!\!\!\int_{m_l m_l' m_s} d\hat{p_1} (lsj, m_l m_s m_j)(l'sj', m_l' m_s m_j') \varphi_{\alpha'}\left(\left|p\hat{p_1} - \frac{1}{2}\vec{q}\right|\right) Y^*_{lm_l}(\hat{p_1}) Y_{l'm_l'}(\widehat{p\hat{p_1} - \frac{1}{2}\vec{q}}). \quad (3.11)$$

Now I take $\vec{q}$ to be in the z-direction to simplify the expression. To make the reasoning behind this clearer, consider $\hat{p_1} = (\sin\theta \cdot \cos\phi, \sin\theta \cdot \sin\phi, \cos\theta)$. By taking $\vec{q}$ to be in the z-direction, I get $p\hat{p_1} - \frac{1}{2}\vec{q} = (p \cdot \sin\theta \cdot \cos\phi, p \cdot \sin\theta \cdot \sin\phi, p \cdot \cos\theta - \frac{1}{2}q)$. Hence, the x- and y-components of $p\hat{p_1} - \frac{1}{2}\vec{q}$ are the same as those of $p\hat{p_1}$. In other words, the ϕ angle of $p\hat{p_1} - \frac{1}{2}\vec{q}$ is the same as that of $\hat{p_1}$. This helps me to separate the $\sin\theta d\theta$ and $d\phi$ integrals of $d\hat{p_1}$. This separation of integrals enables us to make use of the property of spherical harmonics that $\int_0^{2\pi} d\phi Y^*_{lm_l}(\theta, \phi) Y_{l'm_l'}(\theta', \phi) = 2\pi \cdot \delta_{m_l, m_l'}$. Finally, also writing the Kronecker deltas coming from the Clebsch-Gordans, I get

$$= \sum\!\!\!\!\!\!\int_{\alpha'=\{l',s,j',t',m_t',m_j'\}} I \cdot 2\pi \sum\!\!\!\!\!\!\int_{m_l m_l' m_s} \cos\theta d\theta (lsj, m_l m_s m_j)(l'sj', m_l' m_s m_j') \varphi_{\alpha'}\left(\left|p\hat{p_1} - \frac{1}{2}\vec{q}\right|\right) Y^*_{lm_l}(\hat{p_1}) Y_{l'm_l'}(\widehat{p\hat{p_1} - \frac{1}{2}\vec{q}}) \delta_{m_l, m_l'} \delta_{m_l + m_s, m_j} \delta_{m_l' + m_s, m_j'}. \quad (3.12)$$

I substitute $x = \cos\theta$. The Kronecker deltas can be used to eliminate as many quantum

number summations as possible. We finally obtain

$$= \sum\!\!\!\!\!\!\int_{\alpha'=\{l',s,j',t',m'_t,m_j\}} I\cdot 2\pi \sum\!\!\!\!\!\!\int_{m_s} dx(lsj;m_j-m_s,m_s,m_j)(l'sj';m_j-m_s,m_s,m_j)\varphi_{\alpha'}\big(\big|p\hat{p_1}-\frac{1}{2}\vec{q}\big|\big)$$
$$Y^*_{l,m_j-m_s}(\widehat{p_1})Y_{l',m_j-m_s}(\widehat{p\hat{p_1}-\frac{1}{2}\vec{q}}). \quad (3.13)$$

Convection Current Operator

The action of the convection current operator on momentum eigenstates is given by

$$\big\langle \vec{p_1}\big|\vec{j}_c(\vec{q})\big|\vec{p'_1}\big\rangle = \frac{1}{2m_N}\big(\vec{k_1}+\vec{k'_1}\big)\delta^3\big(\vec{k_1}-\vec{k'_1}-\vec{q}\big). \quad (3.14)$$

As can be seen in equation (3.14), the convection current is slightly more complicated to deal with since it contributes more than a simple delta function. It still has no spin dependence and hence is less complicated that the spin current that will be discussed in the next section. This operator contributes in part to the transverse electromagnetic response function of the deuteron. Since the deuteron wave-function is known in the basis $\big|p(ls)jm_jtm_t\vec{P}\big\rangle$, it is the basis I will start the derivation in. The matrix element $\big\langle p(ls)jm_jtm_t\vec{P}\big|\vec{j}^{(1)}_c(\vec{q})\otimes \Pi^{(1)}_{p/n}\big|p'(l's')j'm'_jt'm'_t\vec{P'}\big\rangle$ is given by

$$\big\langle p(ls)jm_jtm_t\vec{P}\big|\vec{j}^{(1)}_c(\vec{q})\otimes\Pi^{(1)}_{p/n}\big|p'(l's')j'm'_jt'm'_t\vec{P'}\big\rangle = \big\langle tm_t\big|\Pi^{(1)}_{p/n}\big|t'm'_t\big\rangle\cdot$$
$$\big\langle p(ls)jm_j\vec{P}\big|\vec{j}^{(1)}_c(\vec{q})\big|p'(l's')j'm'_j\vec{P'}\big\rangle. \quad (3.15)$$

The isospin matrix element $\big\langle tm_t\big|\Pi^{(1)}_{p/n}\big|t'm'_t\big\rangle$ is the same as that from the previous section. I shall deal with this in a later section. Again, as before, we will have to change to a basis where the action of the current operator can be conveniently substituted. To this end, I change to the basis $\big|\vec{p}\vec{P}sm_stm_t\big\rangle$, where the vectors $\vec{p}$ and $\vec{P}$ are the relative and center of mass momentum defined above. This change of basis gives

$$= I\cdot \sum\!\!\!\!\!\!\int_{m_lm'_lm_sm'_s} d^3p_1d^3p_2(lsj,m_lm_sm_j)(l's'j',m'_lm'_sm'_j)\frac{\delta(p-p_1)}{p\cdot p_1}$$
$$\frac{\delta(p'-p_2)}{p'\cdot p_2}\delta_{m_sm'_s}\delta_{ss'}Y^*_{lm_l}(\widehat{p_1})Y_{l'm'_l}(\widehat{p_2})\big\langle\vec{p_1}\vec{P}\big|\vec{j}^{(1)}_c(\vec{q})\big|\vec{p_2}\vec{P'}\big\rangle. \quad (3.16)$$

Here, $\widehat{p}$ represents the angular part of $\vec{p}$. I now substitute the action of the convection current as in equation (3.14) but with the difference that I write it in terms of the relative

and center of mass momenta rather than the individual particle momenta.

$$= I \cdot \sum\!\!\!\!\!\!\int_{m_l m_l' m_s} d^3p_1 d^3p_2 (lsj, m_l m_s m_j)(l's'j', m_l' m_s m_j') \frac{\delta(p-p_1)}{p \cdot p_1} \frac{\delta(p'-p_2)}{p' \cdot p_2} \delta_{ss'}$$
$$Y^*_{lm_l}(\widehat{p_1}) Y_{l'm_l'}(\widehat{p_2}) \frac{1}{2m_N} \left(\frac{\vec{P} + 2\vec{p_1}}{2} + \frac{\vec{P'} + 2\vec{p_2}}{2} \right)$$
$$\delta^3 \left(\frac{\vec{P} + 2\vec{p_1}}{2} - \frac{\vec{P'} + 2\vec{p_2}}{2} - \vec{q} \right) \delta^3 \left(\frac{\vec{P} - 2\vec{p_1}}{2} - \frac{\vec{P'} - 2\vec{p_2}}{2} \right) \quad (3.17)$$

I will use the result of equation (3.17) to calculate the matrix element we are interested in. This matrix element involves the action of the current operator on the deuteron bound state. In the following equation the reasons for the presence integral $\int d^3P$ and for $\vec{P'} = \vec{0}$ are the same as those for the longitudinal current.

$$\int d^3P \left\langle p(ls) j m_j t m_t P \middle| \vec{j}_c^{(1)}(\vec{q}) \otimes \widehat{I}^{(1)} \middle| \Psi \vec{0} \right\rangle = \sum\!\!\!\!\!\!\int_{\alpha' = \{l', s', j', t', m_t', m_j'\}} d^3P \cdot p'^2 dp' \varphi_{\alpha'}(p')$$
$$\left\langle p(ls) j m_j t m_t \vec{P} \middle| \vec{j}_c^{(1)}(\vec{q}) \cdot \widehat{I} \middle| p'(l's') j' m_j' t' m_t' \vec{0} \right\rangle \quad (3.18)$$

Where, $\left|\Psi\vec{0}\right\rangle$ is the deuteron bound state with the centre of mass at rest and $\varphi_{\alpha'}(p') = \left\langle p'\alpha' \middle| \Psi \right\rangle$. Substituting the expression for $\left\langle p(ls) j m_j t m_t \vec{P} \middle| \vec{j}_c^{(1)}(\vec{q}) \cdot \widehat{I} \middle| p'(l's') j' m_j' t' m_t' \vec{0} \right\rangle$ obtained in equation (3.17) I get

$$= \sum\!\!\!\!\!\!\int_{\alpha' = \{l', s', j', t', m_t', m_j'\}} d^3P \cdot p'^2 dp' I \cdot \varphi_{\alpha'}(p') \sum\!\!\!\!\!\!\int_{m_l m_l' m_s} d^3p_1 d^3p_2 (lsj, m_l m_s m_j)$$
$$(l's'j', m_l' m_s m_j') \frac{\delta(p-p_1)}{p \cdot p_1} \frac{\delta(p'-p_2)}{p' \cdot p_2} \delta_{ss'} Y^*_{lm_l}(\widehat{p_1}) Y_{l'm_l'}(\widehat{p_2}) \frac{1}{2m_N} \left(\frac{\vec{P} + 2\vec{p_1}}{2} + \vec{p_2} \right)$$
$$\delta^3 \left(\frac{\vec{P} + 2\vec{p_1}}{2} - \vec{p_2} - \vec{q} \right) \delta^3 \left(\frac{\vec{P} - 2\vec{p_1}}{2} + \vec{p_2} \right). \quad (3.19)$$

I now use delta functions to eliminate the integrals over P, p' and p_2, and I therefore obtain

$$= \sum_{\alpha' = \{l', s', j', t', m_t', m_j'\}} I \cdot \sum\!\!\!\!\!\!\int_{m_l m_l' m_s} d^3p_1 \varphi_{\alpha'}\left(\left| \vec{p_1} - \frac{1}{2}\vec{q} \right| \right) (lsj, m_l m_s m_j)$$
$$(l's'j', m_l' m_s m_j') \frac{\delta(p-p_1)}{p \cdot p_1} \delta_{ss'} Y^*_{lm_l}(\widehat{p_1}) Y_{l'm_l'}\widehat{\left(\vec{p_1} - \frac{1}{2}\vec{q}\right)} \frac{1}{2m_N} (2\vec{p_1}). \quad (3.20)$$

After rewriting the p_1-integral in spherical harmonics as above we obtain

$$= \sum_{\alpha'=\{l',s,j',t',m'_t,m'_j\}} I \cdot \sum\!\!\!\!\!\!\int_{m_l m'_l m_s} d\widehat{p_1}\varphi_{\alpha'}\big(|p\widehat{p_1} - \frac{1}{2}\vec{q}|\big)(lsj, m_l m_s m_j)$$
$$(l'sj', m'_l m_s m'_j) Y^*_{lm_l}(\widehat{p_1}) Y_{l'm'_l}\big(\widehat{p\widehat{p_1} - \frac{1}{2}\vec{q}}\big)\frac{1}{2m_N}(2p\widehat{p_1}). \quad (3.21)$$

I shall consider spherical components of $\vec{j}_c^{(1)}(\vec{q})$. This introduces another spherical harmonic and the parameter λ into the equation. The parameter λ differentiates between the three spherical components of the convection current. It can take values +1, 0 and -1. There are now three spherical harmonics in contrast to the two in the expression for the action of the longitudinal current. The expression becomes

$$\int d^3P \langle p(ls)jm_j tm_t \vec{P}\big|[\vec{j}_c^{(1)}(\vec{q})]^\lambda\big|\Psi\vec{0}\rangle = \sum_{\alpha'=\{l',s,j',t',m'_t,m'_j\}} I \cdot \sum\!\!\!\!\!\!\int_{m_l m'_l m_s} d\widehat{p_1}\varphi_{\alpha'}\big(|p\widehat{p_1} - \frac{1}{2}\vec{q}|\big)$$
$$(lsj, m_l m_s m_j)(l'sj', m'_l m_s m'_j) Y^*_{lm_l}(\widehat{p_1}) Y_{l'm'_l}\big(\widehat{p\widehat{p_1} - \frac{1}{2}\vec{q}}\big)\frac{p}{m_N} Y_{1\lambda}(\widehat{p_1})\sqrt{\frac{4\pi}{3}}. \quad (3.22)$$

Taking $\vec{q}$ to be in the z-direction is beneficial even for the convection current case. Since $\vec{q}$ is in the z-direction, $p\widehat{p_1} - \frac{1}{2}\vec{q}$ will have the same ϕ angle as $\widehat{p_1}$, the ϕ-integral reduces to $2\pi\delta_{m_l,m'_l+\lambda}$ multiplied by the integral over $\cos\theta$.

$$= \sum_{\alpha'=\{l',s,j',t',m'_t,m'_j\}} I \cdot \sum_{m_l m'_l m_s} 2\pi \int_{-1}^{1} dx \varphi_{\alpha'}\big(|p\widehat{p_1} - \frac{1}{2}\vec{q}|\big)(lsj, m_l m_s m_j)(l'sj', m'_l m_s m'_j)$$
$$Y^*_{lm_l}(\widehat{p_1}) Y_{l'm'_l}\big(\widehat{p\widehat{p_1} - \frac{1}{2}\vec{q}}\big)\frac{p}{m_N} Y_{1\lambda}(\widehat{p_1})\sqrt{\frac{4\pi}{3}}\delta_{m_l,m'_l+\lambda} \quad (3.23)$$

In equation (3.23) I substitute $x = \cos\theta$ and eliminate as many quantum number summations as possible using Kronecker deltas arising from the Clebsch-Gordan coefficients. Finally I obtain

$$= \sum_{\alpha'=\{l',s,j',t',m'_t,m_j-\lambda\}} I \cdot \sum_{m_s} 2\pi \int_{-1}^{1} dx \varphi_{\alpha'}\big(|p\widehat{p_1} - \frac{1}{2}\vec{q}|\big)(lsj; m_j - m_s, m_s, m_j)$$
$$(l'sj'; m_j - m_s - \lambda, m_s, m_j - \lambda) Y^*_{l,m_j-m_s}(\widehat{p_1}) Y_{l',m_j-m_s-\lambda}\big(\widehat{p\widehat{p_1} - \frac{1}{2}\vec{q}}\big)\frac{p}{m_N} Y_{1\lambda}(\widehat{p_1})\sqrt{\frac{4\pi}{3}}. \quad (3.24)$$

This is the final expression that I implemented for the action of the convection current operator on deuteron wave function.

Spin Current Operator

The spin current is the other part of the transverse current operator contributing to the transverse response function. The action of the spin current on a momentum eigenstate is given by

$$\langle \vec{p}|\vec{j}_s(\vec{q})|\vec{p'}\rangle = \frac{i}{2m_N}(\vec{\sigma}\times\vec{q})\delta^3(\vec{p}-\vec{p'}-\vec{q}). \tag{3.25}$$

The symbol $\vec{\sigma}$ is the spin operator for spin-1/2 particles, which in cartesian coordinates is $(\sigma_x, \sigma_y, \sigma_z)$, where σ_x, σ_y and σ_z are the three Pauli matrices. This operator is the most complicated to deal with because of the presence of the spin operator and its vector product with $\vec{q}$. I now derive an expression for $\langle p(ls)jm_j tm_t\vec{P}|\vec{j}_s^{(1)}(\vec{q})\otimes\hat{I}^{(1)}|p'(l's')j'm'_j t'm'_t\rangle$. The basis states, isospin matrix element are identical to the previous sections. After a change of basis and substituting the expression resulting from the action of the spin current, I get

$$\begin{aligned}= I\cdot \sum\!\!\!\!\!\!\int_{m_l m_s m'_l m'_s} & d^3p_1 d^3p_2 (lsj; m_l m_s m_j)(l's'j'; m'_l m'_s m'_j)\frac{\delta(p-p_1)}{p\cdot p_1}\frac{\delta(p'-p_2)}{p'\cdot p_2}Y^*_{lm_l}(\widehat{p_1})Y_{l'm'_l}(\widehat{p_2}) \\ & \langle sm_s|\big[\vec{\sigma}^{(1)}\times\vec{q}\big]|s'm'_s\rangle\cdot\frac{i}{2m_N}\delta^3\left(\frac{\vec{P}+2\vec{p_1}}{2}-\frac{\vec{P'}+2\vec{p_2}}{2}-\vec{q}\right)\delta^3\left(\frac{\vec{P}-2\vec{p_1}}{2}-\frac{\vec{P'}-2\vec{p_2}}{2}\right).\end{aligned} \tag{3.26}$$

I now consider the spherical component λ of the current operator. I use $\big[\vec{q}\big]^\lambda = q\sqrt{\frac{4\pi}{3}}Y_{1\lambda}(\widehat{q})$ and $\big[\vec{a}\times\vec{b}\big]^\lambda = -\sqrt{2}i\big\{a,b\big\}^{1\lambda}$. The curly brackets represent coupled tensor operators. The superscript 1λ shows that the coupled tensor operator is of rank 1 and we are dealing with its λ^{th} component.

$$\begin{aligned}= I\cdot \sum\!\!\!\!\!\!\int_{m_l m_s m'_l m'_s} & d^3p_1 d^3p_2 (lsj; m_l m_s m_j)(l's'j'; m'_l m'_s m'_j)\frac{\delta(p-p_1)}{p\cdot p_1}\frac{\delta(p'-p_2)}{p'\cdot p_2}Y^*_{lm_l}(\widehat{p_1}) \\ & Y_{l'm'_l}(\widehat{p_2})\cdot q\sqrt{\frac{8\pi}{3}}\langle sm_s|\big\{\sigma^{(1)},Y_1(\widehat{q})\big\}^{1\lambda}|s'm'_s\rangle \\ & \frac{1}{2m_N}\delta^3\left(\frac{\vec{P}+2\vec{p_1}}{2}-\frac{\vec{P'}+2\vec{p_2}}{2}-\vec{q}\right)\delta^3\left(\frac{\vec{P}-2\vec{p_1}}{2}-\frac{\vec{P'}-2\vec{p_2}}{2}\right)\end{aligned} \tag{3.27}$$

The matrix element $\langle sm_s|\big\{\sigma^{(1)},Y_1(\widehat{q}\big\}^{1\lambda}|s'm'_s\rangle$ shall be derived later. I shall now continue with deriving the action of the spin current on the deuteron bound state. In the following

derivation $\varphi_{\alpha'}(p') = \langle p'\alpha'|\Psi\rangle$ as before.

$$\int d^3P \langle p(ls)jm_j tm_t P|\vec{J}_s^{(1)}(\vec{q})\otimes\widehat{I}^{(1)}|\Psi\vec{0}\rangle = \sum\!\!\!\!\!\!\int_{\alpha'=\{l',s',j',m'_j,t',m'_t\}} d^3P\cdot p'^2 dp'\varphi_{\alpha'}(p')I\cdot$$

$$\sum\!\!\!\!\!\!\int_{m_l m_s m'_l m'_s} d^3p_1 d^3p_2 (lsj;m_l m_s m_j)(l's'j';m'_l m'_s m'_j)\frac{\delta(p-p_1)}{p\cdot p_1}\frac{\delta(p'-p_2)}{p'\cdot p_2}Y^*_{lm_l}(\widehat{p_1})Y_{l'm'_l}(\widehat{p_2})$$

$$\cdot q\sqrt{\frac{8\pi}{3}}\langle sm_s|\{\sigma^{(1)},Y_1(\widehat{q})\}^{1\lambda}|s'm'_s\rangle\frac{1}{2m_N}\delta^3\left(\frac{\vec{P}+2\vec{p_1}}{2}-\vec{p_2}-\vec{q}\right)\delta^3\left(\frac{\vec{P}-2\vec{p_1}}{2}+\vec{p_2}\right) \quad (3.28)$$

Exactly like the longitudinal and convection currents, I use delta functions to eliminate from the expression the integrals over P, p' and p_2. I then split the integral over p_1 into magnitude and angular parts. This step is followed by taking $\vec{q}$ in z-direction. I get

$$= \sum_{\alpha'=\{l',s',j',m'_j,t',m'_t\}} I\cdot \sum\!\!\!\!\!\!\int_{m_l m_s m'_l m'_s} d\widehat{p_1}\varphi_{\alpha'}\left(|p\widehat{p_1}-\frac{1}{2}\vec{q}|\right)(lsj;m_l m_s m_j)(l's'j';m'_l m'_s m'_j)$$

$$Y^*_{lm_l}(\widehat{p_1})Y_{l'm'_l}\widehat{\left(p\widehat{p_1}-\frac{1}{2}\vec{q}\right)}\cdot q\sqrt{\frac{8\pi}{3}}\langle sm_s|\{\sigma^{(1)},Y_1(\widehat{q})\}^{1\lambda}|s'm'_s\rangle\frac{1}{2m_N}. \quad (3.29)$$

As before, $\vec{q}$ is in the z-direction. The right hand side simplifies as follows:

$$= \sum_{\alpha'=\{l',s',j',m'_j,t',m'_t\}} 2\pi I\cdot \sum\!\!\!\!\!\!\int_{m_l m_s m'_l m'_s} dx\varphi_{\alpha'}\left(|p\widehat{p_1}-\frac{1}{2}\vec{q}|\right)(lsj;m_l m_s m_j)(l's'j';m'_l m'_s m'_j)$$

$$Y^*_{lm_l}(\widehat{p_1})Y_{l'm'_l}\widehat{\left(p\widehat{p_1}-\frac{1}{2}\vec{q}\right)}\cdot q\sqrt{\frac{8\pi}{3}}\langle sm_s|\{\sigma^{(1)},Y_1(\widehat{q})\}^{1\lambda}|s'm'_s\rangle\frac{1}{2m_N}\delta_{m_l m'_l} \quad (3.30)$$

I will now derive the expression for the spin matrix element. In the spin matrix element $\langle sm_s|\{\sigma^{(1)},Y_1(\widehat{q})\}^{1\lambda}|s'm'_s\rangle$ the spins of the nucleons (1/2 each) are coupled. The operators $\sigma^{(1)}$ and $Y_1(\widehat{q})$ are also coupled. I first decouple the operators using Clebsch-Gordan coefficients.

$$\langle sm_s|\{\sigma^{(1)},Y_1(\widehat{q})\}^{1\lambda}|s'm'_s\rangle = \sum_\mu (111;\lambda-\mu,\mu,\lambda)Y_{1\mu}(\hat{q})\langle sm_s|[\sigma^{(1)}]^{1,\lambda-\mu}|s'm'_s\rangle \quad (3.31)$$

In the previous equation, the spin states are coupled but the operator $[\sigma^{(1)}]^{1,\lambda-\mu}$ acts only on the 1st particle. This operator can be considered to be coupled with the operator 1. We

then evaluate the matrix element using the Wigner-Eckart theorem. This leads to

$$\left\langle sm_s\middle|\left\{\sigma^{(1)},Y_1(\widehat{q})\right\}^{1\lambda}\middle|s'm'_s\right\rangle = \sum_{\mu}(111;\lambda-\mu,\mu,\lambda)Y_{1\mu}(\widehat{q})\sqrt{\widehat{\frac{1}{2}}\widehat{\frac{1}{2}}\widehat{1}\widehat{s'}}\begin{Bmatrix}1/2 & 1/2 & 1\\ 1/2 & 1/2 & 0\\ s & s' & 1\end{Bmatrix} (s'1s;m'_s,\lambda-\mu,m_s)\left\langle 1/2\middle\|\sigma^{(1)}\middle\|1/2\right\rangle. \quad (3.32)$$

In the previous equation, the matrix element $\left\langle 1/2\middle\|\sigma^{(1)}\middle\|1/2\right\rangle$ is a reduced matrix element. I define reduced matrix elements as follows:

$$\left\langle j'm'\middle|T^q_k\middle|jm\right\rangle = (jkj';mqm')\left\langle j'\middle\|T_k\middle\|j\right\rangle \quad (3.33)$$

where m' and m are the third components of j' and j. The operator T^q_k is the q^{th} component of a tensor operator of rank k. Also, the expression enclosed in curly brackets is a 9j-symbol. The notation $\hat{a}$ for quantum numbers means $2a+1$. To simplify equation (3.32) I use $\left\langle 1/2\middle\|\sigma^{(1)}\middle\|1/2\right\rangle = \sqrt{3}$. Furthermore, we can use Kronecker deltas arising from the Clebsch-Gordan coefficients to eliminate quantum number summations. For the spin matrix element, I finally obtain

$$= 6(111;m_s-m'_s,\lambda+m'_s-m_s,\lambda)Y_{1,m'_s-m_s+\lambda}(\widehat{q})\sqrt{\widehat{s'}}\begin{Bmatrix}1/2 & 1/2 & 1\\ 1/2 & 1/2 & 0\\ s & s' & 1\end{Bmatrix} (s'1s;m'_s,m_s-m'_s,m_s). \quad (3.34)$$

I now continue with the derivation of the spin current by using the result from (3.34) in (3.30). In the spin current case, an additional consequence of taking $\vec{q}$ in the z-direction is that I can write $Y_{1,m'_s-m_s+\lambda}(\widehat{q}) = \sqrt{\frac{\widehat{1}}{4\pi}}\cdot\delta_{m'_s-m_s+\lambda,0}$. I therefore obtain

$$\int d^3P\left\langle p(ls)jm_jtm_tP\middle|\vec{j}^{(1)}_s(\vec{q})\otimes\widehat{I}^{(1)}\middle|\Psi\vec{0}\right\rangle = \sum_{\alpha'=\{l',s',j',m'_j,t',m'_t\}} 2\pi I\cdot \sum\!\!\!\!\!\!\int_{m_lm_sm'_lm'_s} dx$$

$$\varphi_{\alpha'}\left(\left|p\widehat{p_1}-\frac{1}{2}\vec{q}\right|\right)(lsj;m_lm_sm_j)(l's'j';m'_lm'_sm'_j)Y^*_{lm_l}(\widehat{p_1})Y_{l'm'_l}\widehat{\left(p\widehat{p_1}-\frac{1}{2}\vec{q}\right)}\cdot q\sqrt{\frac{8\pi}{3}}6$$

$$(111;m_s-m'_s,\lambda+m'_s-m_s,\lambda)\sqrt{\frac{\widehat{1}}{4\pi}}\cdot\delta_{m'_s-m_s+\lambda,0}$$

$$\sqrt{\widehat{s'}}\begin{Bmatrix}1/2 & 1/2 & 1\\ 1/2 & 1/2 & 0\\ s & s' & 1\end{Bmatrix}(s'1s;m'_s,m_s-m'_s,m_s)\frac{1}{2m_N}\delta_{m_lm'_l}. \quad (3.35)$$

Additional Kornecker deltas are obtained form the Clebsch-Gordans which eliminate many sums over quantum numbers. We finally obtain

$$= \sum_{\alpha'=\{l',s',j',m_j-\lambda,t',m_t'\}} 12\sqrt{2}\pi\sqrt{\widehat{s'}} I \cdot \sum\!\!\!\!\!\!\int_{m_s} dx \phi_{\alpha'}\big(\big|p\widehat{p_1} - \frac{1}{2}\vec{q}\big|\big)(lsj; m_j - m_s, m_s, m_j)$$

$$(l's'j'; m_j - m_s, m_s - \lambda, m_j - \lambda) Y^*_{l,m_j-m_s}(\widehat{p_1}) Y_{l',m_j-m_s}\big(\widehat{p\widehat{p_1} - \frac{1}{2}\vec{q}}\big) \cdot q(111; \lambda, 0, \lambda)$$

$$\begin{Bmatrix} 1/2 & 1/2 & 1 \\ 1/2 & 1/2 & 0 \\ s & s' & 1 \end{Bmatrix} (s'1s; m_s - \lambda, \lambda, m_s) \frac{1}{2m_N}. \quad (3.36)$$

Isospin Matrix Element

In this section I shall derive in short the expression for the isospin matrix element I. Nucleons have isospin $1/2$ with the proton having z-component $+1/2$ and neutron with z-component $-1/2$. In the basis I have used, the individual nucleon isospins are coupled to give a total isospin for the two-nucleon system. The isospin projection operator $\Pi^{(1)}_{p/n}$ projects a given single particle isospin state $\big|\frac{1}{2}m_t\big\rangle_{(1)}$ on to a proton/neutron. The isospin projection operator for a proton/neutron is

$$\Pi^{(1)}_{p/n} = \frac{1}{2}(1 \pm \tau^{(1)}_3) F^{p/n} \quad (3.37)$$

where $F^{p/n}$ is the appropriate proton/neutron form factor according to the type of current operator we are interested in. The operator $\tau^{(1)}_3$ is a tensor operator acting on the 1^{st} particle. We are interested in computing the matrix element $\big\langle tm_t\big|\frac{1}{2}(1 \pm \tau^{(1)}_3)\big|t'm_t'\big\rangle$. The operator 1 is a scalar operator and gives $\delta_{m_t,m_t'}\delta_{t,t'}$. The operator $\tau^{(1)}_3$ is a tensor operator and is more complicated to deal with. To compute this operator, I make use of the Wigner-Eckart theorem

$$\big\langle tm_t\big|\frac{1}{2}\tau^{(1)}_3\big|t'm_t'\big\rangle = \frac{1}{2}\big(t', 1, t; m_t', 0, m_t\big)\big\langle t\big\|\tau^{(1)}_3\big\|t'\big\rangle. \quad (3.38)$$

The reduced matrix element $\big\langle t\big\|\tau^{(1)}_3\big\|t'\big\rangle$ has coupled states and the operator $\tau^{(1)}_3$ can be considered to be coupled with the operator 1. This leads to a further simplification as

follows:

$$\left\langle tm_t\right|\frac{1}{2}\tau_3^{(1)}\left|t'm_t'\right\rangle = \frac{1}{2}6\cdot\sqrt{\hat{t}'}\cdot\left(t',1,t;m_t',0,m_t\right)\begin{Bmatrix}1/2 & 1/2 & 1\\ 1/2 & 1/2 & 0\\ t & t' & 1\end{Bmatrix} \underbrace{\left\langle 1/2\middle\|\tau_3^{(1)}\middle\|1/2\right\rangle}_{\sqrt{3}}\underbrace{\left\langle 1/2\middle\|1\middle\|1/2\right\rangle}_{1}. \quad (3.39)$$

Therefore, the isospin matrix element becomes

$$\begin{aligned}\left\langle tm_t\right|\Pi_p^{(1)}+\Pi_n^{(1)}\left|t'm_t'\right\rangle &= \left\langle tm_t\right|\frac{1}{2}((F^p+F^n)+(F^p-F^n)\tau_3^{(1)})\left|t'm_t'\right\rangle\\ &= \left(\delta_{m_t,m_t'}\delta_{t,t'}\frac{F^p+F^n}{2}+6\frac{F^p-F^n}{2}\cdot\sqrt{\hat{t}'}\cdot\left(t',1,t;m_t',0,m_t\right)\begin{Bmatrix}1/2 & 1/2 & 1\\ 1/2 & 1/2 & 0\\ t & t' & 1\end{Bmatrix}\right). \quad (3.40)\end{aligned}$$

The expressions $\frac{F^p+F^n}{2}$ and $\frac{F^p-F^n}{2}$ are called isoscalar and isovector form factors respectively.

3.2. Integral Transforms of the Response Function

As mentioned in the introduction, a direct calculation of the response function would involve the calculation of scattering states. This approach is impractical for large nuclei. An easier approach is to calculate the integral transforms of the response function using bound state techniques. In this thesis I deal with the Stieltjes and Lorentz transforms of the response function. The Stieltjes and Lorentz transforms of the response functions are performed with integration kernels $\frac{1}{\omega+\sigma}$ and $\frac{1}{(\omega-\sigma_R)^2+\sigma_I^2}$ respectively. As will be shown below, one can formulate dynamical equations for both cases that allow one to obtain the transformed response only using bound state techniques.

Stieltjes Transform

To derive an expression for the Stieltjes transform of the response functions in terms of current operator matrix elements, I begin with the definition of the longitudinal response function. The extension to the transversal case is straightforward and will not be explicitly repeated here.

$$R(\omega,\vec{q}) = \frac{1}{3}\sum_{m_f m_i}\int df\,\delta(-\omega+E_f-E_i)\left|\left\langle m_f\phi\middle|j^0(\vec{q})\middle|\Psi m_i\right\rangle\right|^2 \quad (3.41)$$

Here, $E_i = -|E_d|$ and $|\Psi m_i\rangle$ is the deuteron bound state with third component of total angular momentum m_i and $E_f = E_f^{rel} + \frac{Q^2}{2m_N}$. E_d is the binding energy of the deuteron. E_f^{rel} is the final relative energy of the two nucleon system. $|m_f \phi\rangle$ is the state of the two-nucleon system after inelastic scattering. m_f is the z-component of the total angular momentum of the outgoing state respectively. The Stieltjes transform of the response function is defined as

$$\Phi_S(\sigma) = \int_{\omega_0}^{\infty} d\omega \frac{R(\omega, \vec{Q})}{\omega + \sigma}. \tag{3.42}$$

We are interested in inelastic scattering, E_f^{rel} is the relative energy transferred to the two-nucleon system. We are only interested in studying reactions involving break-up. The lowest value of E_f^{rel} for which there is break-up of the deuteron is $\omega_0 = |E_d| + \frac{Q^2}{2m_N}$, hence the response function is zero for $\omega < \omega_0$. Using the delta function in equation (3.41) to eliminate the ω-integral, the Stieltjes transformed response function becomes

$$\Phi(\sigma) = \frac{1}{3} \sum_{m_i} \int df \langle \Psi m_i | j^{0\dagger}(\vec{q}) | m_f \phi \rangle \frac{1}{E_f^{rel} + \omega_0 + \sigma} \langle m_f \phi | j^0(\vec{q}) | \Psi m_i \rangle. \tag{3.43}$$

The integral $\int df$ is over all final unbound states, since we are dealing with the break-up of the deuteron. This integral over unbound states can replaced by an integral over all states and subtract a summation over bound states. In the two-nucleon case, we can have bound states with different z-components of total angular momentum. The integral over all final states can be absorbed into the unity operator. We therefore obtain

$$= \frac{1}{3} \sum_{m_i} \Bigg(\langle \Psi m_i | j^{0\dagger}(\vec{q}) \frac{1}{H + \omega_0 + \sigma} j^0(\vec{q}) | \Psi m_i \rangle - \langle \Psi m_i | j^{0\dagger}(\vec{q}) | \Psi m_i \rangle \frac{1}{-|E_d| + \omega_0 + \sigma} \langle \Psi m_i | j^0(\vec{q}) | \Psi m_i \rangle \Bigg). \tag{3.44}$$

The Stieltjes transform can be defined as $\frac{1}{3} \sum_{m_i} \langle \Psi m_i | j^{0\dagger}(\vec{q}) | m_i \Phi \rangle$, where

$$|m_i \Phi\rangle = -\Bigg(G(-\omega_0 - \sigma) + |\Psi m_i\rangle \frac{1}{-|E_d| + \omega_0 + \sigma} \langle \Psi m_i | \Bigg) j^0(\vec{q}) | \Psi m_i \rangle. \tag{3.45}$$

This expression uses the full and free resolvent operators, $G(z) = \frac{1}{-H+z}$ and $G_0 = \frac{1}{-H_0+z}$. By making use of the resolvent identity $G = G_0 + G_0 V G$ and $G(-\omega_0 - \sigma) j^0(\vec{q}) | \Psi m_i \rangle =$

$-\big|m_i\Phi\big\rangle - \Big(\big|\Psi m_i\big\rangle \frac{1}{-|E_d|+\omega_0+\sigma}\big\langle\Psi m_i\big|\Big) j^0(\vec{q})\big|\Psi m_i\big\rangle$ I find

$$\big|m_i\Phi\big\rangle = -G_0(-\omega_0-\sigma)j^0(\vec{q})\big|\Psi m_i\big\rangle + G_0(-\omega_0-\sigma)V\big|m_i\Phi\big\rangle + G_0(-\omega_0-\sigma)V\frac{\big|\Psi m_i\big\rangle\big\langle\Psi m_i\big|}{-|E_d|+\omega_0+\sigma} j^0(\vec{q})\big|\Psi m_i\big\rangle - \frac{\big|\Psi m_i\big\rangle\big\langle\Psi m_i\big|}{-|E_d|+\omega_0+\sigma} j^0(\vec{q})\big|\Psi m_i\big\rangle. \quad (3.46)$$

In order to be able to use the Schrödinger equation $G_0(-|E_d|)V\big|\Psi m_i\big\rangle = \big|\Psi m_i\big\rangle$, we rewrite $G_0(-\omega_0-\sigma) = G_0(-|E_d|) + G_0(-\omega_0-\sigma)(-|E_d|+\omega_0+\sigma)G_0(-|E_d|)$.

$$\begin{aligned}\big|m_i\Phi\big\rangle - G_0(-\omega_0-\sigma)V\big|m_i\Phi\big\rangle = {} & -G_0(-\omega_0-\sigma)j^0(\vec{q})\big|\Psi m_i\big\rangle + G_0(-|E_d|)V\frac{\big|\Psi m_i\big\rangle\big\langle\Psi m_i\big|}{-|E_d|+\omega_0+\sigma} \\ & j^0(\vec{q})\big|\Psi m_i\big\rangle + G_0(-\omega_0-\sigma)(-|E_d|+\omega_0+\sigma)G_0(-|E_d|)V\frac{\big|\Psi m_i\big\rangle\big\langle\Psi m_i\big|}{-|E_d|+\omega_0+\sigma} \\ & j^0(\vec{q})\big|\Psi m_i\big\rangle - \frac{\big|\Psi m_i\big\rangle\big\langle\Psi m_i\big|}{-|E_d|+\omega_0+\sigma} j^0(\vec{q})\big|\Psi m_i\big\rangle \quad (3.47)\end{aligned}$$

The above equation has the form of an inhomogeneous Schrödinger-like equation. All the energies involved in the t-matrix and the propagators are negative, which avoids singularities. The inhomogeneous part contains the deuteron bound state which is known. Using $(1+G_0t)(1-G_0V) = 1$ we get

$$\big|m_i\Phi\big\rangle = \Big(1+G_0(-\sigma-\omega_0)t(-\sigma-\omega_0)\Big)G_0(-\sigma-\omega_0)\Big(-1+\big|\Psi m_i\big\rangle\big\langle\Psi m_i\big|\Big)j^0(\vec{q})\big|\Psi m_i\big\rangle. \quad (3.48)$$

Note that all terms involving the deuteron pole are canceled in this final expression. For $\sigma > 0$, none of the terms involve a singularity. Therefore, the equation can be solved using standard bound state techniques.

Lorentz Transform

The Lorentz transform of the response function is defined as

$$\Phi_L(\sigma_R,\sigma_I) = \int_0^\infty d\omega \frac{R(\omega,\vec{Q})}{(\sigma_R-w)^2+\sigma_I^2}. \quad (3.49)$$

We need an expression for the Lorentz transform in terms of the current operator matrix elements. Again, we derive the equations for the case of the longitudinal response. From

the definition, we have

$$\Phi_L(\sigma) = \int_0^\infty d\omega \frac{\frac{1}{3}\sum_{m_f m_i} \int df \delta(-\omega + E_f^{rel} + \omega_0) \left| \langle m_f \phi | j^0(\vec{q}) | \Psi m_i \rangle \right|^2}{(\omega - \sigma_R)^2 + \sigma_I^2}. \tag{3.50}$$

,where $\sigma = \sigma_R + i\sigma_I$. The extension to the transversal case is obvious. As in the previous subsection we can rewrite the integral over the final unbound states as an integral over all final states minus a sum over bound states with all possible spins.

$$\Phi_L(\sigma) = \frac{1}{3}\sum_{m_i} \Bigg(\langle \Psi m_i | j^{0\dagger}(\vec{q}) \cdot \frac{1}{H + \omega_0 - \sigma_R + i\sigma_I} \cdot \frac{1}{H + \omega_0 - \sigma_R - i\sigma_I} \cdot j^0(\vec{q}) | \Psi m_i \rangle \\ - \langle \Psi m_i | j^{0\dagger}(\vec{q}) | \Psi m_i \rangle \cdot \frac{1}{(E_f^{rel} + \omega_0 - \sigma_R)^2 + \sigma_I^2} \cdot \langle \Psi m_i | j^0(\vec{q}) | \Psi m_i \rangle \Bigg) \tag{3.51}$$

The Lorentz transform can be defined as $\frac{1}{3}\sum_{m_i} \langle m_i \Phi | m_i \Phi \rangle$ where $|m_i\Phi\rangle = \left(\frac{1}{H+\omega_0-\sigma} - \frac{|\Psi m_i\rangle\langle\Psi m_i|}{-|E_d|+\omega_0-\sigma} \right) j^0(\vec{q}) |\Psi m_i\rangle$. We therefore have for $|m_i\Phi\rangle$

$$|m_i\Phi\rangle = \left(- G_0(\sigma - \omega_0) - G_0(\sigma - \omega_0) V G(\sigma - \omega_0) - \frac{|\Psi m_i\rangle\langle\Psi m_i|}{-|E_d| + \omega_0 - \sigma} \right) j^0(\vec{q}) |\Psi m_i\rangle. \tag{3.52}$$

After steps similar to the previous section, we arrive at the following inhomogeneous equation:

$$|m_i\Phi\rangle = \Big(1 + G_0(\sigma - \omega_0) t(\sigma - \omega_0)\Big) G_0(\sigma - \omega_0) \Big(-1 + |\Psi m_i\rangle\langle\Psi m_i| \Big) j^0(\vec{q}) |\Psi m_i\rangle. \tag{3.53}$$

This is equation is very similar to equation (3.48) derived for the Stieltjes-transform. Note that here, σ enters with the opposite sign. Nevertheless singularities do not show up since σ is now complex. To avoid singularities, the imaginary part of σ must be chosen large enough. Besides that, the energies become complex. The equation can once again be solved using standard bound state techniques.

So far I have derived all the expressions necessary for the calculation of the Stieltjes or Lorentz transform of response functions driven by various currents, when the bound-state wave-function is known. With the knowledge of the integral transforms, the response function can be obtained by solving an ill-posed problem. I shall discuss the set-up and methods for solving the ill-posed problem in the next chapter.

4. Back Transformations

The previous chapter contains all the information necessary to calculate the Stieltjes and Lorentz transforms of the electromagnetic response functions of the deuteron. In this chapter I shall discuss in detail the process by which the response function is determined from its integral transforms. As mentioned earlier, the problem of finding the response functions with the knowledge of its integral transforms is an ill-posed one. By "Back Transformation", I mean the act of solving the said inverse problem. So far in the literature, basis functions have been used for the purpose of the back-transformation, e.g. [12]. The basis functions approach depends heavily on the choice of basis functions. This choice introduces a bias in the response function that is eventually calculated. In this thesis I replaced the basis functions approach with a more systematic approach that avoids this bias. Multiple techniques were used to perform the back transformation, each of which has a number of parameters. These techniques were tested on a case where the analytical expression for the exact response function was known.

4.1. Discretisation of Integral Transforms

In this section I shall describe the inverse problem that needs to be solved. In order to set-up the problem, we look at the discretisation of the integral transforms. A typical discretisation of a general integral transform of the response function is given by,

$$\Phi(\sigma_i, \vec{Q}) = \sum_{j=0}^{n} \kappa_{ij} R(\omega_j, \vec{Q}) \cdot q_j \tag{4.1}$$

In equation (4.1), q_j is the integration weight corresponding to ω_j and κ_{ij} is the kernel of the integral transform. It is equal to $\frac{1}{\omega_j + \sigma_i}$ and $\frac{1}{(\omega_j - \sigma_{R_i})^2 + \sigma_I^2}$ for the Stieltjes and Lorentz transform respectively. Define $\vec{\Phi} \in \mathbb{R}^m$, $\vec{R} \in \mathbb{R}^n$, and $K \in \mathbb{R}^{m \times n}$ such that

$$\Phi_i = \Phi(\sigma_i, \vec{Q}) \tag{4.2}$$

$$R_i = R(\omega_i, \vec{Q}) \tag{4.3}$$

and

$$K_{ij} = \kappa_{ij} \cdot q_j \tag{4.4}$$

Hence, we have the matrix equation

$$\vec{\Phi} = K \cdot \vec{R} \tag{4.5}$$

In this thesis, I have performed a combined Lorentz- and Stieltjes-Transformed analysis of the response function. For this purpose, the vector $\vec{\Phi}$ and the matrix K are taken as follows.

$$\vec{\Phi} = \begin{pmatrix} \Phi_S \\ w_L \cdot \Phi_L \end{pmatrix} \tag{4.6}$$

$$K = \begin{pmatrix} K_S \\ w_L \cdot K_L \end{pmatrix} \tag{4.7}$$

In the above two equations, the subscripts S and L stand for the Stieltjes and Lorentz transforms respectively. w_L is a weighting factor given to the Lorentz transform. Since all numbers in the vector $\vec{\Phi}$ should have the same unit, the Lorentz weight w_L should have appropriate units. The Stieltjes and Lorentz transform have the units fm^{-1} and fm^{-2}, respectively. Therefore, the Lorentz weight w_L should have the unit fm. The matrix K and the vector $\vec{\Phi}$ are already known. As mentioned earlier, the problem of finding R in the above equation is an ill posed problem.

4.2. Back Transformation Techniques

The equation (4.5) is what is called as a linear inverse problem. These are often ill-posed. In our case, this is so because the integral transforms mentioned smooth out the sharp features of the response function. The matrix K can in general be rank deficient (the range of the matrix is a subset of $\mathbb{R}^m$). In such a case there is no vector $\vec{R}$ that exactly solves equation (4.5). If the matrix K is rectangular but of rank m, the equation has an infinite number of solutions. In such cases the solution vector $\vec{R}$ can be defined as one that "solves" the problem in a least squares sense. We can define the solution to be a vector for which

$$\|K\vec{R} - \vec{\Phi}\|_2 \to min \tag{4.8}$$

and

$$\|\vec{R}\|_2 \to min \tag{4.9}$$

hold simultaneously. Hence $\vec{R}$ is called a least squares solution. This way of defining a solution has a problem. Let $\vec{\Phi}'$ denote an integral transform with some error. Let $\vec{R}'$ be the least squares solution obtained from the erroneous integral transform. For an ill-posed inverse problem, depending on the matrix, a small error in the integral transform $\|\vec{\Phi} - \vec{\Phi}'\|$ leads to a very large error in the response function $\|\vec{R} - \vec{R}'\|$. Hence better definitions of the least squares solution are needed. Methods that deal with such problems make use of the "Singular Value Decomposition" (SVD) of the matrix K.

Singular Value Decomposition (SVD)

Every matrix $K \in \mathbb{R}^{m\times n}$ has a singular value decomposition given by

$$K = U \cdot \Sigma \cdot V^T \tag{4.10}$$

where $U = \left[\vec{u}_1 \cdots \vec{u}_m\right]$, $v = \left[\vec{v}_1 \cdots \vec{v}_n\right]$ are orthogonal matrices [17]. The vectors $\vec{u}_i, i \in 1,..,m$ and $\vec{v}_i, i \in 1,..,n$ are called the left and right singular vectors of the matrix K, respectively. They form orthonormal bases of $\mathbb{R}^m$ and $\mathbb{R}^n$ respectively. Σ is a diagonal matrix $\in \mathbb{R}^{m\times n}$ which contain the singular values of the matrix K. If $m < n$ $\Sigma = \begin{bmatrix} \alpha_1 & \cdots & 0 & \cdots & 0 \\ \vdots & \ddots & \vdots & \ddots & \vdots \\ 0 & \cdots & \alpha_m & \cdots & 0 \end{bmatrix}$, and if $m > n$ $\Sigma = \begin{bmatrix} \alpha_1 & \cdots & 0 \\ \vdots & \ddots & \vdots \\ 0 & \cdots & \alpha_n \\ \vdots & \ddots & \vdots \\ 0 & \cdots & 0 \end{bmatrix}$. Here, $\alpha_1, .., \alpha_{min\{m,n\}}$ are the singular values of the matrix K which are non-negative for real matrices. The singular values and the corresponding singular vectors are arranged such that $\alpha_1 \geq \alpha_2 \geq \cdots \geq \alpha_{min\{m,n\}}$.

Now consider a general linear inverse problem involving matrix K, $K\vec{R} = \vec{\Phi}$. The least squares solution defined earlier using relations (4.8) and (4.9) is given using the SVD of matrix K as,

$$\vec{R} = \sum_{i=1}^{r} \frac{\vec{\Phi} \cdot \vec{u}_i}{\alpha_i} \vec{v}_i \tag{4.11}$$

Here, r is the number of nonzero singular values of the matrix K. Such a solution is highly sensitive to errors if the error in $\vec{\Phi}$ is dominated by vectors $\vec{u}_i$ which correspond to the smallest non zero singular values of the matrix K. This tells us that all singular values of the matrix K should not be given the same importance. Better solutions use so called regularisation methods for the SVD. These regularisation methods are described below.

4.2.1. Truncated Singular Value Decomposition (TSVD)

The TSVD method has been described in [9]. This regularisation method involves discarding singular values of the matrix K that are smaller than a pre-determined cutoff. Given the singular value decomposition of K we can find $\vec{R}$ as

$$\vec{R} = \sum_{i=0}^{r} a_i \vec{v}_i \tag{4.12}$$

Where

$$a_i = \begin{cases} 0 & \text{for } \frac{|\alpha_i|}{\alpha_{max}} < \epsilon \text{ (SVD truncation parameter)} \\ \frac{\phi_i}{\alpha_i} & \text{otherwise, with } \phi_i = \vec{\Phi} \cdot \vec{u}_i \end{cases}. \tag{4.13}$$

In this regularisation method, one has the freedom of choosing the parameter ϵ. A large value of epsilon makes sure that the smaller singular values have no impact on the solutions. In many cases it is the smallest non zero singular values that are responsible for error magnification. If ϵ is chosen too large, we ignore the larger singular values which directly correspond to the left singular vectors that hold the largest information in the vector Φ. This loss of information again causes the solution to be meaningless. Hence, an optimal choice of the truncation parameter ϵ is necessary. In section 4.3, I present the results of my study of the optimal choice for ϵ.

4.2.2. Tikhonov Regularisation (TR)

In this method we use a continuous function to filter the singular values of the matrix. Given the singular value decomposition of K we can find $\vec{R}$ as

$$\vec{R} = \sum_{i=0}^{r} h_\mu(\alpha_i)(\vec{\Phi} \cdot \vec{u}_i)\vec{v}_i \tag{4.14}$$

where, $h_\epsilon(s) = \frac{s^2}{s^2+\mu^2}$ and μ is the regularisation parameter [16].

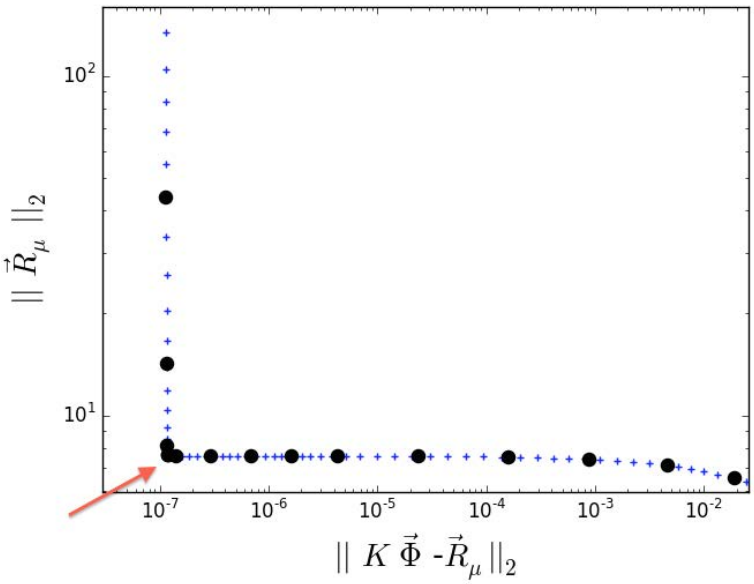

Figure 4.1.: A typical L-curve

Unlike for the TSVD regularisation method, there is, in the literature, a heuristic method to determine the optimal value of the regularisation parameter μ [8]. It is called the L-curve method. In this method, the points $(\|K\vec{R}_\mu - \vec{\Phi}\|_2, \|\vec{R}_\mu\|_2)$ are plotted for various values of

the regularisation parameter μ on a logarithmic scale. Heuristically, the optimal ϵ is the one that corresponds to the bent region of the L-curve.

The figure 4.1 shows an L-curve obtained using data from the test case described in the next section. According to the heuristic, the optimum μ is the one corresponding to the bend in the L-curve. The bend is marked in the figure with a red arrow. There are comments on my attempt to use the L-curve method for response functions in section 4.3.

Throughout the remaining part of the thesis, the parameter ϵ shall be associated with the TSVD method and μ will be associated with the TR method.

4.3. Stability of Back Transformation Techniques

In this section I shall compare the different methods which can be used to recover the response function for a test case. The test case was the longitudinal s-wave deuteron response function for the Yamaguchi potential [19]. This test case was chosen since the exact expression for the s-wave response function is known. A derivation of this response function can be found in [13]. A plot of the exact response function is shown in figure 4.2. I also attempt to find optimal values of the parameters involved. I performed the stability analysis in three cases:

1. Using the Stieltjes-transformed response function.

2. Using the Lorentz-transformed response function.

3. Using both the Lorentz- and Stieltjes-transforms of the response function.

The Stieltjes- and Lorentz-transforms of the response function shown in figure 4.2 are show in figures 4.3 and 4.4, respectively. The difference in the maximum values of the two functions is to be noted. This difference in magnitude will be used to find an appropriate value for the Lorentz weight in Chapter 5.

In each of the above cases I use both TSVD and TR to solve the inverse problem. I used the method L-curves to attempt to find an optimum μ for the back-transformation with TR. As mentioned earlier, one of the L-curves obtained for the test case is shown in figure 4.1. For this particular L-curve, μ was varied from 1 to 3.16228×10^{-10}. The black dots are the points corresponding to $\mu = 1.0$, $\mu = 3.16228 \times 10^{-1}$, $\mu = 1.0 \times 10^{-2}$ and so on. The attempt was unsuccessful because the value of μ suggested by the L-curve did not yield a good estimate for the response function. I therefore decided to explicitly compare response functions obtained using different ϵ and μ values. In order to compare the different estimates of the response function obtained, I needed to define a suitable measure for the quality of

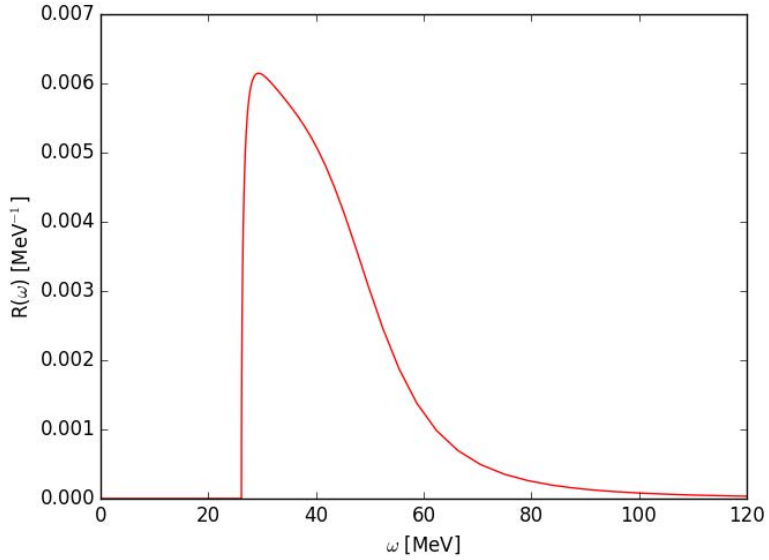

Figure 4.2.: Exact Response Fucntion for the Test Case $|\vec{Q}| = 300$ MeV

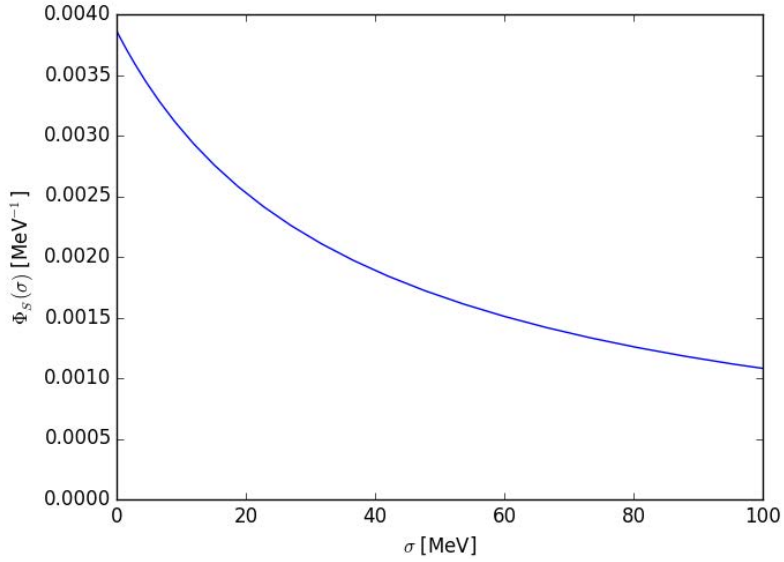

Figure 4.3.: Stieltjes Transform of the Response Function $|\vec{Q}| = 300$ MeV

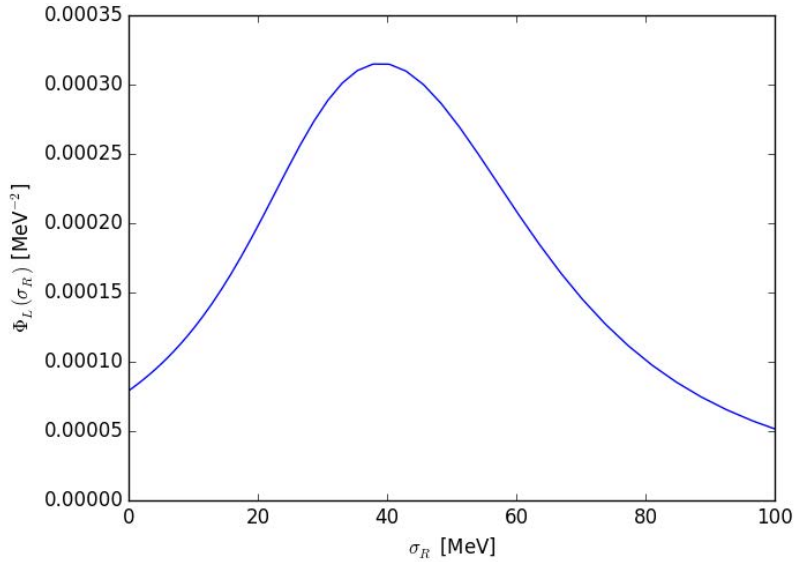

Figure 4.4.: Lorentz Transform of the Response Function $|\vec{Q}| = 300$ MeV and $\sigma_I = 0.1$ fm

the response function. I defined the following error function:

$$Error = \sqrt{\frac{1}{N_\omega}\sum_{i=1}^{N_\omega}(R_{bt}(\omega_i) - R_{exact}(\omega_i))^2} \tag{4.15}$$

Here R_{bt} is the back transformed response function. I chose this error because the value of the response function falls very fast with increasing ω. The most important features of the response function are in the range of low ω. Hence this definition of the error, which makes the values of the response function in the lower range of ω more important. To find the optimum ϵ and μ I plotted the back transform error vs the number of σ or σ_R grid points for different values of ϵ or μ. The expectation was, that for an optimum ϵ or μ the back transform error will be the lowest and will converge to some constant value as the number of σ grid points is increased. The value of ϵ or μ that would satisfy this expectation would be chosen as the optimum. This is the method used to find the optimum ϵ or μ for all test cases. As we will see in plots in the last subsection of the chapter, errors of 10^{-2} fm and lower generally correspond to response functions which are optically very similar to the one in figure 4.2.

For the back-transform, the number of grid points on the ω grid had to be decided. I chose the grid points such that the Stieltjes- and Lorentz-transforms of the s-wave response function were converged to machine precision. The number of ω grid points thus determined was 300. The number of σ and σ_R grid points was varied. Throughout the study I choose the magnitude of photon momentum $|\vec{Q}|$ to be 300 MeV.

4.3.1. Stieltjes-Transformed Analysis

For the case where only the Stieltjes-transformed response function is used, the parameters that can be controlled are the σ grid and the SVD regularisation parameter. I used the TSVD method and TR method. I made plots, as I mentioned earlier, to find the optimum values of ϵ and μ. These are shown in figures 4.5 and 4.6.

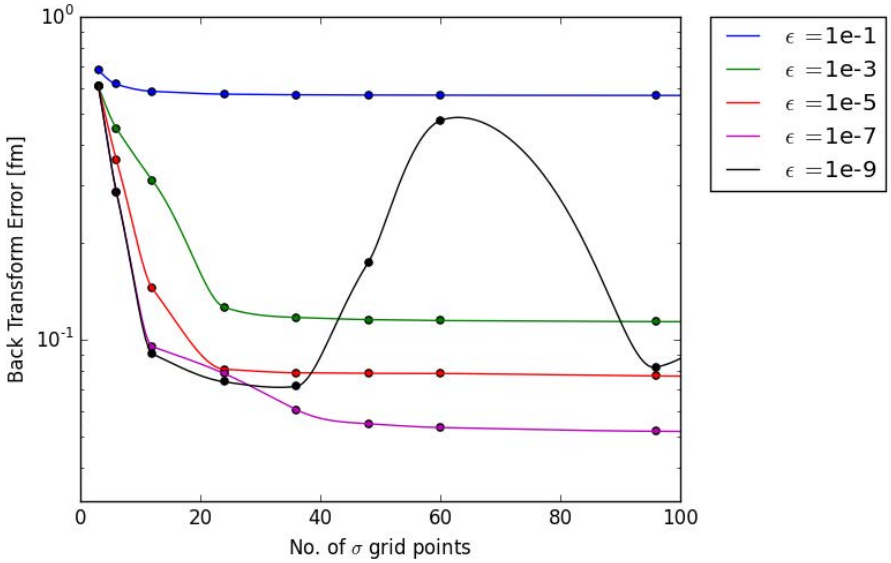

Figure 4.5.: The Stieltjes transform of the response function is used. The back transformation error defined in equation (4.15) is plotted versus the number of σ grid points for different TSVD truncations ϵ. The lines are to guide the eye.

In figures 4.5 and 4.6, it can be seen that the back transform error reduces with the number of mesh points at first. For the larger values of ϵ or μ the back-transform error stabilises approximately above 20 to 30 σ grid points. For very small values of ϵ or μ there is no stable plateau region for a larger number σ grid points. These points were considered unsuitable for the back-transformation. Of the values of ϵ or μ for which the back-transform error is stable, I chose the one for which the converged error is minimum. Using this argument, the best values of ϵ and μ are 10^{-7} and 10^{-5} respectively.

I shall now compare the response functions obtained from each of the previous cases against the exact response function. In figures 4.7 and 4.8, I show the response functions with the least errors, obtained from the Stieltjes transform, using TSVD and TR respectively. The errors in the back transformed response functions are $5 \cdot 10^{-2}$ fm and $7 \cdot 10^{-2}$ fm. It can be seen that, though the shape of the response functions is somewhat similar to the exact one, the response function obtained from TSVD becomes negative in the ω region after about

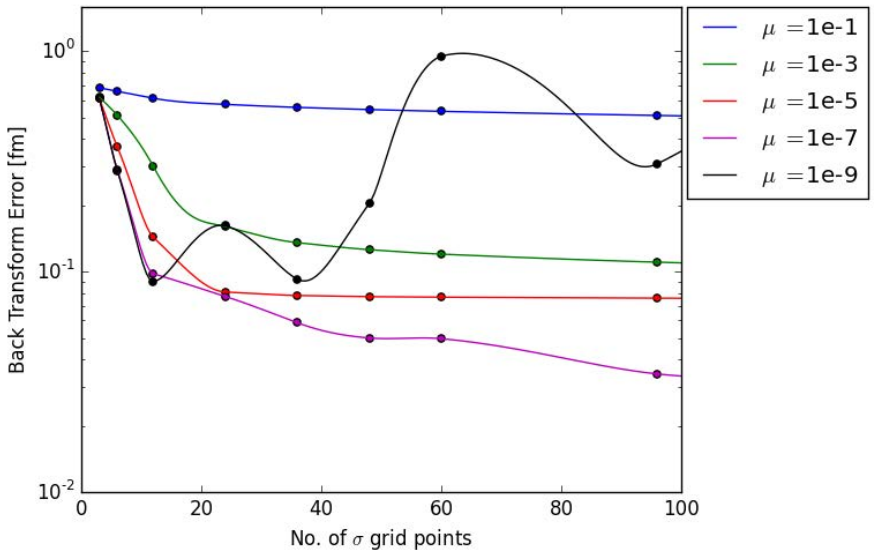

Figure 4.6.: The Stieltjes transform of the response function is used. The back transformation error defined in equation (4.15) is plotted versus the number of σ grid points for different TR parameters μ. The lines are to guide the eye.

80 MeV. This effect is much less pronounced in the response function obtained from TR. However, with both methods, the results are not sufficiently accurate.

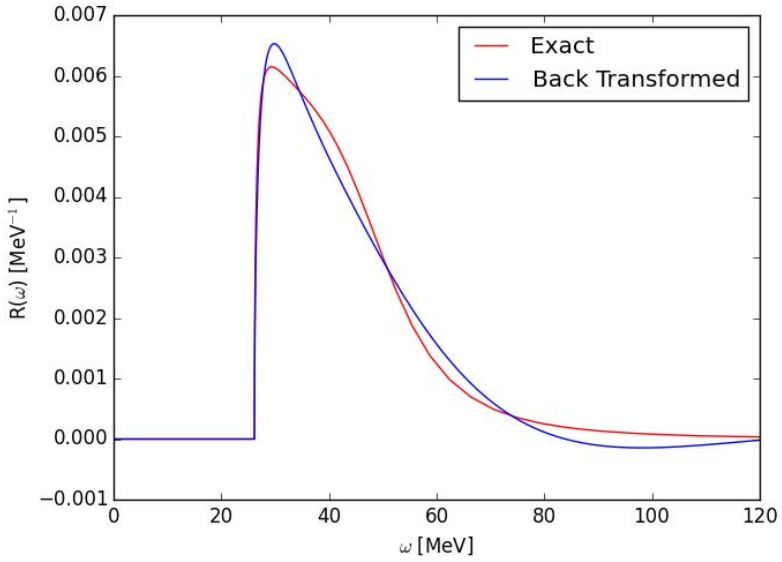

Figure 4.7.: Response function obtained from the Stieltjes-transform compared with the exact response function of figure 4.2. The TSVD method was used for the back transformation with $\epsilon = 10^{-7}$ and $N_\sigma = 36$, with $|\vec{Q}| = 300$ MeV.

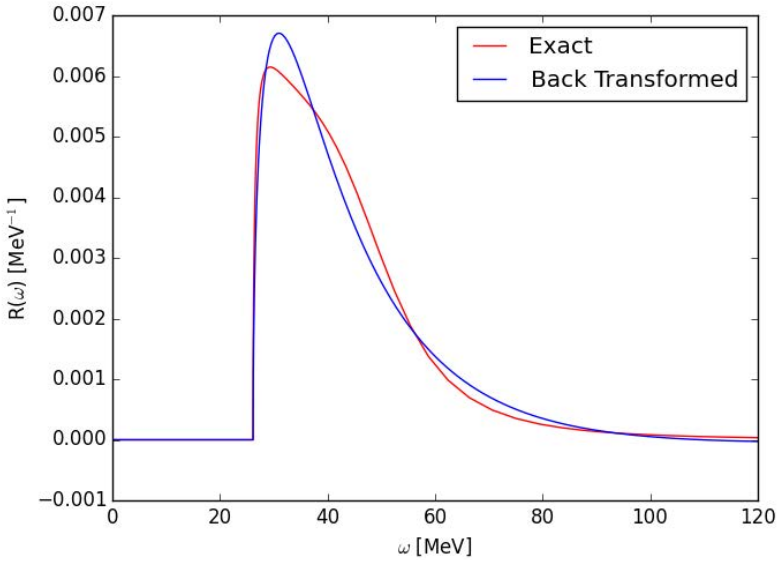

Figure 4.8.: Response function obtained from the Stieltjes-transform compared with the exact response function of figure 4.2. The TR method was used for the back transformation with $\mu = 10^{-5}$ and $N_\sigma = 36$, with $|\vec{Q}| = 300$ MeV

4.3.2. Lorentz-Transformed Analysis

With the Lorentz-transform, there is an additional parameter involved, i.e. the imaginary part σ_I. This parameter controls how blurred the response function becomes after the integral transformation. As σ_I tends to zero, the back transform becomes theoretically easier since the Lorentz-transform is exactly like the response function, but numerically, this becomes very hard to deal with because of singularities. So an optimum value of σ_I needs to be found. I have performed trials with two values of σ_I, 1.0 fm^{-1}, and 0.1 fm^{-1}. A similar procedure as the one described in the last Subsection was used to find the optimum values of the regularisation parameters (ϵ and μ). The values thus found for the Lorentz transform case are given in table 4.1.

	$\sigma_I = 0.1$ fm^{-1}	$\sigma_I = 1.0$ fm^{-1}
ϵ	10^{-7}	10^{-7}
μ	10^{-5}	10^{-7}

Table 4.1.: Optimal ϵ and μ for Lorentz Transform case

Figures 4.9 and 4.10 show the best response functions obtained from the Lorentz-transform at $\sigma_I = 1.0$ fm^{-1}. One can see that again the outcome is not sufficiently similar to the exact response function of figure 4.2. In fact, the oscillations in the tail are even more pronounced than for the Stieltjes case. On the other hand, TR and TSVD result in very similar response functions. The errors defined in equation (4.15) in both the response functions are around 0.1 fm in both cases.

Next, I present in figures 4.11 and 4.12 the response functions obtained using the two methods (TSVD and TR) but using the Lorentz transform at $\sigma_I = 0.1$ fm^{-1}. These response functions are in much better agreement with the exact one. Both the errors are around 10^{-2} fm. The Lorentz transform is certainly better for the purpose of back transformation than the Stieltjes transform. Nevertheless, there are very slight oscillations in both plots which were absent in the Stieltjes case. This different behaviour of the back-transformed response function is the motivation behind investigating the effectiveness of a combined Lorentz- and Stieltjes-transformed analysis.

For $\sigma_I = 1.0$ fm^{-1} I was able the obtain an accuracy of 6 significant digits for the Lorentz-transform of the response function. For $\sigma_I = 0.1$ fm^{-1} the accuracy was reduced to 5 significant digits. σ_I was reduced further by an order of magnitude but it was observed that this made it hard to achieve an accuracy of 5 significant digits and hence the attempt was abandoned. It is clear from these trials that $\sigma_I = 1.0$ fm^{-1} is not a suitable value to calculate the Lorentz-transform of the response function. Henceforth, if the value of σ_I is not mentioned in discussions involving the Lorentz-transform, it can be assumed that $\sigma_I = 0.1$ fm^{-1}.

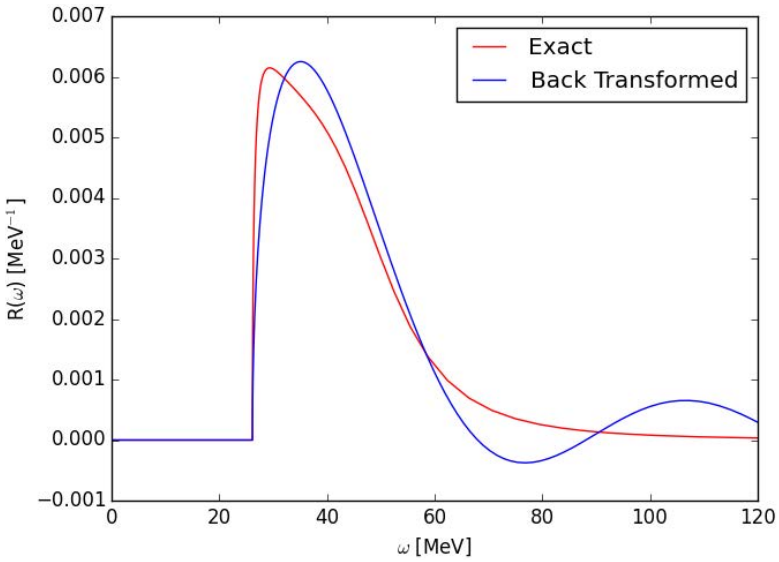

Figure 4.9.: Response function obtained from the Lorentz-transform ($\sigma_I = 1.0$ fm^{-1}) compared with the exact response function of figure 4.2. The TSVD method was used for the back transformation with $\epsilon = 10^{-7}$ and $N_\sigma = 36$, with $|\vec{Q}| = 300$ MeV

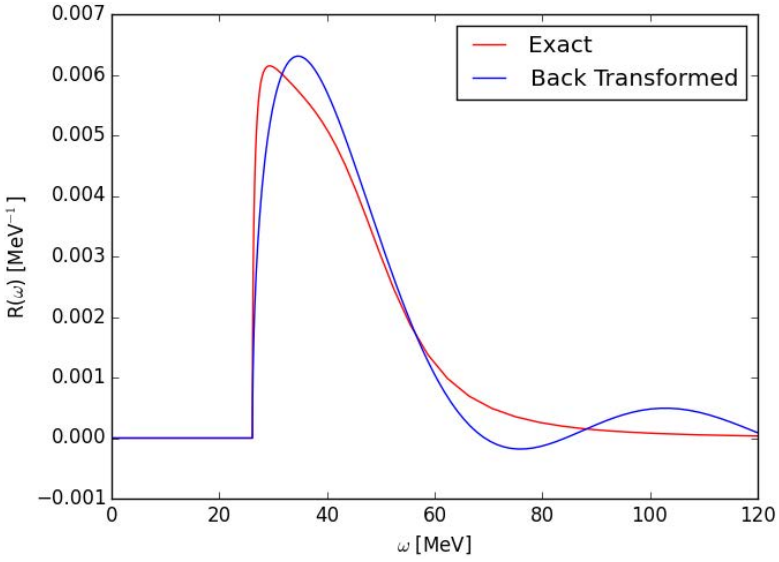

Figure 4.10.: Response function obtained from the Lorentz-transform ($\sigma_I = 1.0$ fm^{-1}) compared with the exact response function of figure 4.2. The TR method was used for the back transformation with $\mu = 10^{-7}$ and $N_\sigma = 36$, with $|\vec{Q}| = 300$ MeV

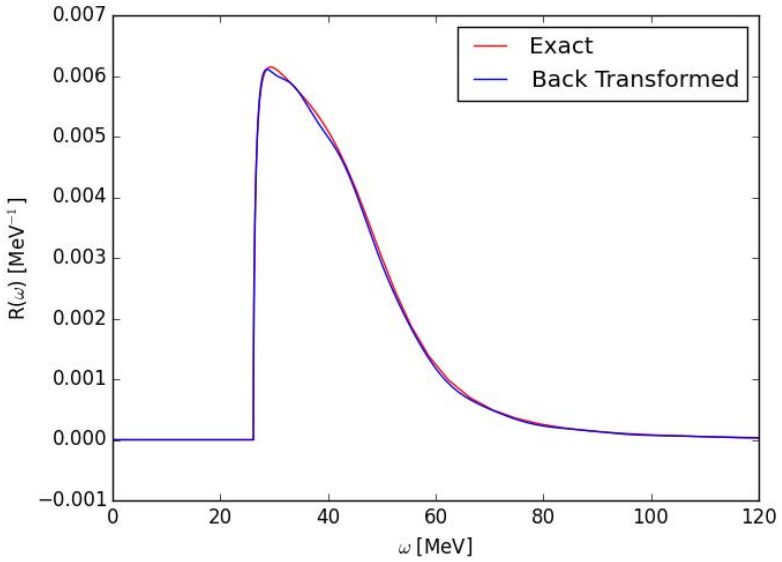

Figure 4.11.: Response function obtained from the Lorentz-transform ($\sigma_I = 0.1$ fm^{-1}) compared with the exact response function of figure 4.2. The TSVD method was used for the back transformation with $\epsilon = 10^{-7}$ and $N_\sigma = 36$, with $|\vec{Q}| = 300$ MeV

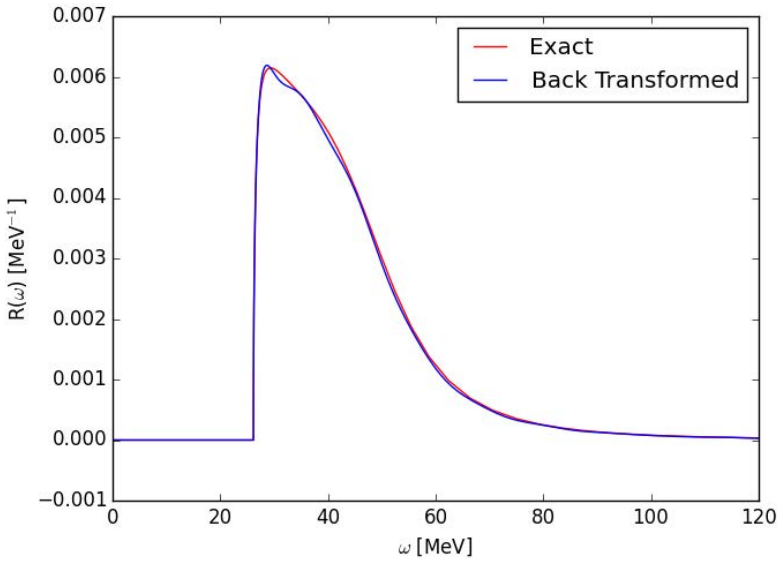

Figure 4.12.: Response function obtained from the Lorentz-transform ($\sigma_I = 0.1$ fm^{-1}) compared with the exact response function of figure 4.2. The TR method was used for the back transformation with $\mu = 10^{-5}$ and $N_\sigma = 36$, with $|\vec{Q}| = 300$ MeV

4.3.3. Combined Lorentz- and Stieltjes-Transformed Analysis

As mentioned earlier, the motivation for carrying out a combined analysis is the fact that the back transformed response functions obtained from the Stieltjes and Lorentz transform have different types of discrepancies in them when compared to the exact response function. The response function that comes from the Stieltjes transform tends to become negative for larger values of ω whereas the one that comes from the Lorentz transform tends to have oscillations.

For the case where both integral transforms are used, I gave a weight of 1 fm to the Lorentz transform ($w_L = 1$ fm). The optimum values of ϵ and μ were 10^{-5} and 10^{-3} respectively. In figures 4.13 and 4.14 are shown the response functions obtained using both integral transforms from the TSVD method and the TR method, respectively. From the figures it can be seen that the oscillations in the back-transformed response function are of a very low frequency. This is in contrast to the response functions obtained using only the Lorentz transform. Another point to be noted is that the the back-transformed response functions always remain positive. Hence we can say that the using both integral transforms of the response function has enabled us to eliminate the adverse effects of using both transforms by themselves. Unfortunately, a new feature appears that adversely affects the quality of the response function. This is a sort of a depression in the response function just right of the peak. This feature is more prominent in the TSVD case in figure 4.13.

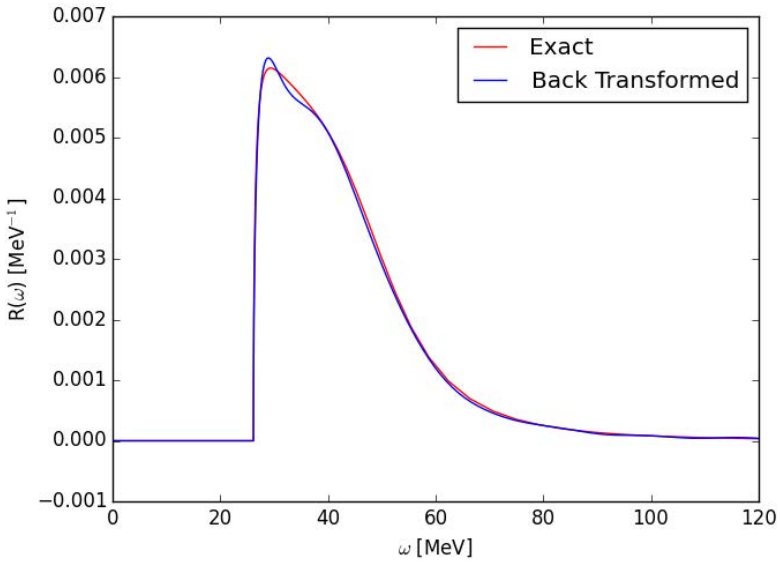

Figure 4.13.: Response function obtained using both integral transforms ($\sigma_I = 0.1$ fm^{-1}) compared with the exact response function of figure 4.2. The TSVD method was used for the back transformation with $\epsilon = 10^{-5}$ and $N_\sigma = 36$, with $|\vec{Q}| = 300$ MeV

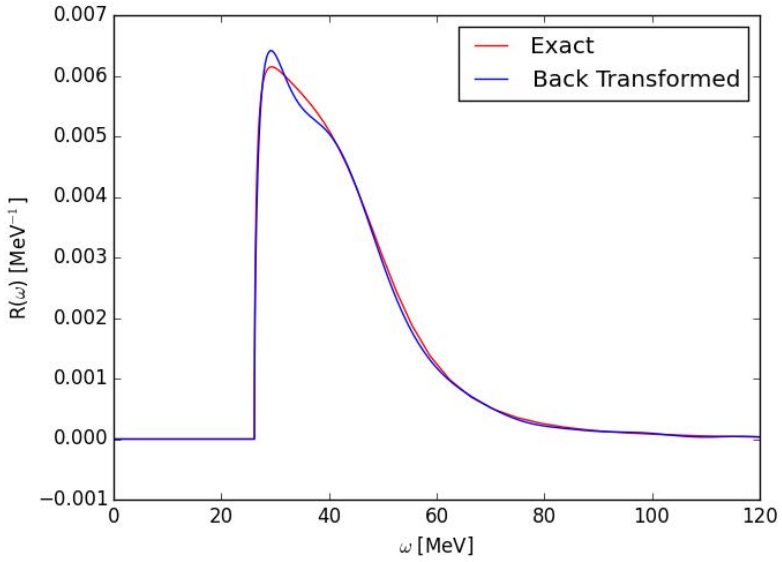

Figure 4.14.: Response function obtained using both integral transforms ($\sigma_I = 0.1$ fm^{-1}) compared with the exact response function of figure 4.2. The TR method was used for the back transformation with $\mu = 10^{-3}$ and $N_\sigma = 36$, with $|\vec{Q}| = 300$ MeV

5. Results

In the last chapter, I discussed in more detail a test case for which I new the exact result. Now I switch to a more realistic case where the exact result is not known a priori. Nevertheless, I will show how to find the best parameters for the back transformation in a systematic way. I will also try to get an estimate of the uncertainty of the calculated response functions by variations of the parameters.

Although I once again restrict myself to 1-nucleon current operators, the application of a realistic potential involves the full complexity of a nuclear system. Due to the tensor interaction of the realistic potential, partial wave channels are coupled. Additionally, I consider longitudinal and transverse currents.

For the test case in the last chapter, I used a Lorentz weight $w_L = 1.0$ fm. Since the relative magnitudes of the Stieltjes and Lorentz transforms are different, it makes more sense to choose a Lorentz weight that takes this information into consideration. The use of different Lorentz weights w_L is also discussed below.

I have calcuted estimates of the longitudinal and transverse electromagnetic response functions of the deuteron using the Nijmegen93 potential [15]. Since analytical expressions for the response functions are not known in this case, the method used in the previous chapter to determine an optimum ϵ or μ cannot be used here. I first noted the response function for a particular value of ϵ or μ. Next, I changed the ϵ or μ to 3 times the original value. I then calculated the norm of the difference between the two response functions thus obtained ($||R_\epsilon - R_{3\epsilon}||$ or $||R_\mu - R_{3\mu}||$) for different numbers of σ grid points. The expectation was, that for an optimum value of ϵ or μ, the following two conditions would be satisfied:

1. the norm would be stable with respect to the number of σ grid points, and

2. the norm would be the smallest among the converged ones.

The TSVD method cannot be used in this case because of the discrete cutoff for singular values. TR is better suited in for this case since it has a continuously varying filter function for the singular values. In the last chapter, It was observed that both TSVD and TR methods worked equally well to extract the response function, so I decided to use only the TR method for the realistic case.

In section 4.3 the Lorentz weight w_L was chosen to be 1 fm. In this chapter I will also investigate the effects of changing this parameter.

In figure 5.1 the μ dependence of the result is shown. This plot is for the case in which the Stieltjes transform of the longitudinal response function is used. For the Lorentz-transform and combined-transforms cases, I found a similar behaviour of the differences of the back-transformation results for different μ. We see that $||R_\mu - R_{3\mu}||$ is stable with respect to the number of σ grid points for $\mu = 10^{-1}$ and $\mu = 10^{-7}$. Since, in the stable region, $||R_\mu - R_{3\mu}||$ is smaller for $\mu = 10^{-7}$, I chose $\mu = 10^{-7}$ as the optimum value of μ for this case. I did not choose $\mu = 10^{-5}$ because the difference of the back-transformation result is steadily rising with an increase in N_σ. The optimum values of μ obtained using only the Stieltjes transform or only the Lorentz transform with this method are given in table 5.1.

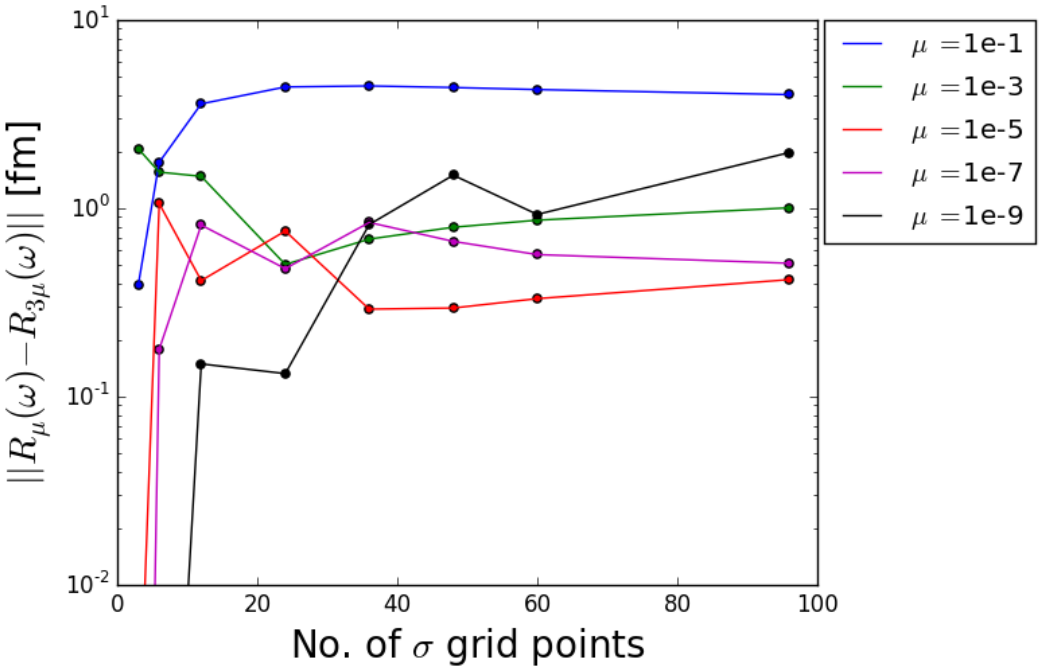

Figure 5.1.: Deviation of different back transforms obtained from the Stieltjes transform. Calculations performed for $|\vec{Q}| = 300$ MeV.

For the combined back-transformation, we first need to fix the relative weight with which both transformations contribute. The motivation behind choosing a Lorentz weight different from 1 fm is that the maximum values of the Lorentz and Stieltjes transforms of the response function differ by orders of magnitude. My starting point for the choice of the relative weight is a factor w_L chosen such that the maximum of the transformed functions is approximately

	Longitudinal	Transverse
Stieltjes	10^{-7}	10^{-7}
Lorentz	10^{-3}	10^{-3}

Table 5.1.: Optimal μ using one integral transform at a time

equal hoping that this leads to an approximately equal influence of both transformations on the result. With this in mind, I chose the Lorentz weights as the ratio between the maximum values of the Lorentz and Stieltjes transforms of the longitudinal and transverse response functions. The Lorentz weights for the longitudinal and transverse cases were found to be $w_L = 0.08334$ fm and $w_L = 0.041667$ fm, respectively. Additionally, I attempted back transformations for half and twice these values. For each case, I have then found optimal μ as described above. The results for these optimal μ are summarised in Table 5.2.

	Longitudinal $w_L = 0.08334$ fm	Transverse $w_L = 0.041667$ fm
$0.5 \cdot w_L$	10^{-3}	10^{-5}
w_L	10^{-3}	10^{-3}
$2 \cdot w_L$	10^{-3}	10^{-5}

Table 5.2.: Optimal μ for both integral transforms for different Lorentz weights

Once the the regularisation parameter μ is determined, the back transformation using TR gives us no error bars. Ideally, it would be beneficial to have some idea about the possible variation in the back-transformed response function. To this end, I performed the back transformation for the optimum μ, $\frac{1}{3} \cdot \mu$ and $3 \cdot \mu$. I then calculated the maximum and minimum values among the three response functions for each ω point. Plotting the maximum and minimum on the same axes gives us a band that indicates the uncertainty of the results. This gives us a way to estimate the variation in the back-transformed response function. These band plots for the longitudinal and transverse response functions obtained using different methods are given in figures 5.2 and 5.3.

The Stieltjes transforms of the longitudinal and transverse response functions were calculated with an accuracy of 6 significant digits, whereas the Lorentz transforms of both response functions have an accuracy of 5 significant digits.

I will first discuss my results for the longitudinal response function. Figure 5.2 shows the results of the longitudinal response function based on the different integral transforms. I begin with the discussion of the results obtained using only the Stieltjes transform. Note that the thickness of the band for the only-Stieltjes case is large in the region of the peak and in the high energy tail. This reflects high uncertainties in the peak and tail. Besides, the peak height and the high ω behaviour largely deviates from the other cases of Figure 5.2. It can also be seen that part of the band becomes negative for some large ω. A

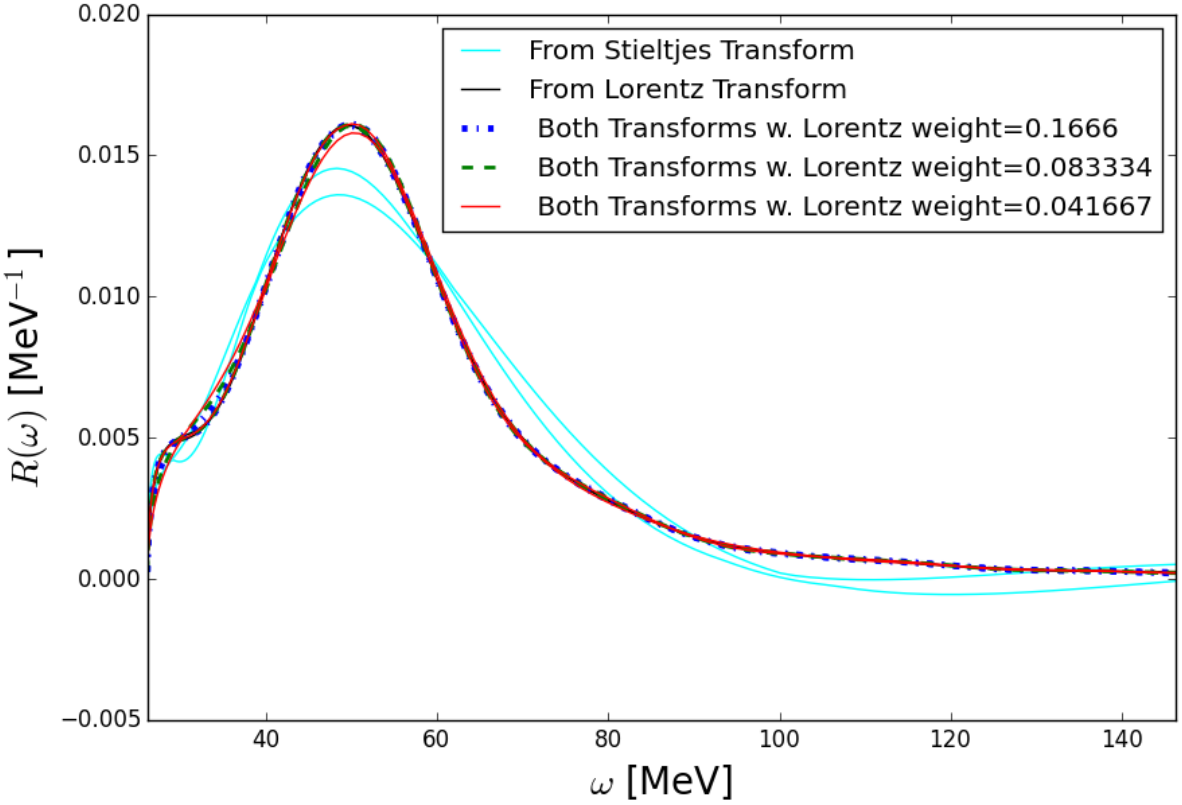

Figure 5.2.: Results for the longitudinal response function. The values of the μ for the five cases in the legend are 10^{-7}, 10^{-3}, 10^{-3}, 10^{-3}, and 10^{-3}, respectively. The maximum and minimum values among $\{R_{\frac{1}{3}\mu}(\omega), R_{\mu}(\omega), R_{3\mu}(\omega)\}$ for all the different μ are plotted for each value of ω. $|\vec{Q}|$ is chosen as 300 MeV, and $N_\sigma = 36$.

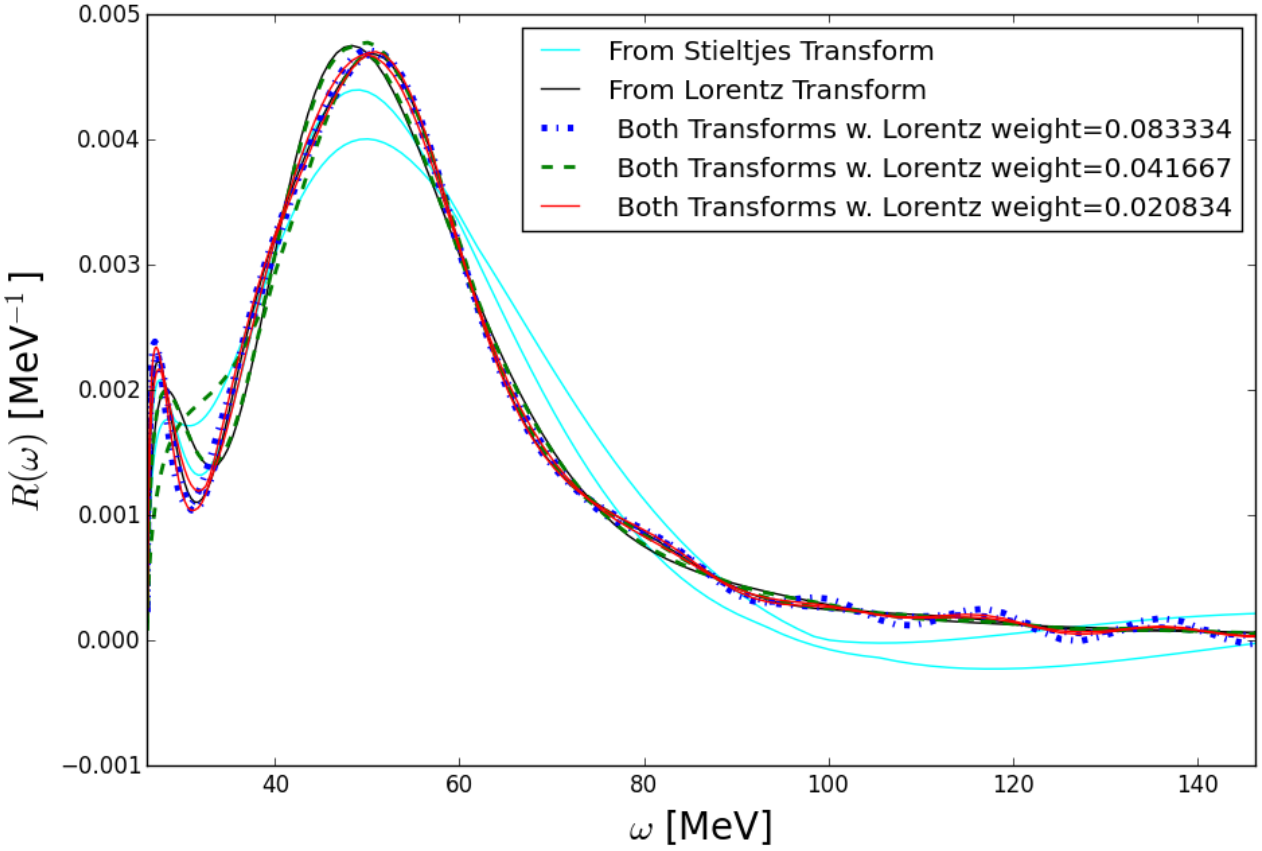

Figure 5.3.: Results for the transverse response function. The values of the μ for the five cases in the legend are 10^{-7}, 10^{-3}, 10^{-5}, 10^{-3}, and 10^{-5}, respectively. The maximum and minimum values among $\{R_{\frac{1}{3}\mu}(\omega), R_{\mu}(\omega), R_{3\mu}(\omega)\}$ for all the different μ are plotted for each value of ω. $|\vec{Q}|$ is chosen as 300 MeV, and $N_\sigma = 36$.

physically correct response function should be free from oscillations, and non-negative in the complete ω range. I now turn to the estimate of the response function based on the Lorentz-transform. Here, we see a very thin band for the longitudinal response function. Its thickness too small to be noticed optically for most ω. This suggests a low uncertainty and hence high reliability for this particular result. I shift my focus to the response function estimates obtained using a combination of both integral transforms. This result contains three response functions obtained with the relative weights $w_L = 0.1666$ fm, $w_L = 0.083334$ fm, and $w_L = 0.041667$ fm. The width of the band is highest for $w_L = 0.041667$ fm and the lowest for $w_L = 0.1666$ fm. For $w_L = 0.1666$ fm the width of the band of the response function is too small to be noticed. The results based on the Lorentz transform and that based on the combined transforms for the case of $w_L = 0.1666$ fm mostly overlap. In addition to the overlap, the absence of oscillations and the non negativity suggest that these results are more physically correct. Since, using only the Lorentz transform resulted in a very reliable estimate, one can expect larger relative weights for the Lorentz transform to work better when both integral transforms are used. Using both integral transforms to obtain the response function is effective in getting an estimate with low uncertainty. Even though using the Lorentz transform alone has the same effect, using both integral transforms certainly better than using the Stieltjes transform alone. From the more reliable estimates of the response function we can see that the longitudinal response function first has a shoulder in the region around $\omega = 30$ MeV, followed by a peak of height ≈ 0.016 MeV^{-1} and then a tail region in which it asymptotically goes to zero.

I will now turn my attention to the results of the transverse response function. In Figure 5.3 we have the transverse response function based on the different integral transforms. For the result obtained only using the Stieltjes transform, we again see a band of large thickness in the region of the peak and in the high energy tail. Again the peak height and the high ω behaviour is totally inconsistent with the other results of Figure 5.3. The minimum estimate for the response function becomes negative for large ω. I now move on to the Lorentz transform based result. This result shows a thinner band than the Stieltjes case but its width is still noticeable. There are also some oscillations in the high ω region. Here, unlike in the longitudinal response function case, neither integral transform used by itself can yield a response with negligibly low uncertainty. I now consider the transverse response function based on the combined integral transforms. Here, again, we have response functions for three different relative weights $w_L = 0.083344$ fm, $w_L = 0.041667$ fm, and $w_L = 0.020834$ fm. We see here that the largest width of the band exists for $w_L = 0.041677$ fm. The other two Lorentz weight give a smaller width for the band, which is even smaller than the estimate obtained using the Lorentz transform alone. This is different from the case of Figure 5.2, where the one of the extreme values of w_L corresponded to the largest uncertainty estimate. For $w_L = 0.083334$ fm and $w_L = 0.020834$ fm the plots mostly overlap only deviating from each other slightly in the tail. The two bands mostly overlap in the low ω region but the oscillations in the tail are of a slightly higher amplitude for the case of $w_L = 0.083344$ fm. This is a reliable result and is a significant improvement over the cases where only one integral transform. It can be concluded, that in the case

of the transverse response function, using both integral transforms to obtain the response function is the more successful strategy. Note that the transverse response function has a local minimum approximately in the region where the longitudinal response function has a shoulder. Around 20 MeV, the transverse response function also has a small peak. The asymptotic behaviour in the high ω region is common to both response functions.

These examples conclude the first application of our back-transformation scheme based on Stieltjes-, Lorentz- and combined transformations. Except for the only-Stieltjes case, we obtained consistent and stable results in both cases, the longitudinal and transverse response functions. Thereby, we have not introduced any bias due to a special basis for the back transformation. The combination of Lorentz- and Stieltjes- was especially important for the transversal case. Interestingly we were able to observe a very narrow structure at low ω for this case, which is consistently reproduced for all examples we considered. Further applications of this new scheme will be very interesting in the future.

6. Conclusion

In this thesis I have analysed inclusive electron-scattering on a two-nucleon system.

In chapter 2 I have approximated the cross-section for inelastic inclusive scattering by a 1-photon exchange. Furthermore, I treat the interaction of the photon and nucleons as if the nucleons behave like free particles. By doing so, I have neglected the so called "exchange currents" which arise from the interaction of the photon with the pions which mediate the interaction between nucleons. Through this approximation I have replaced the nucleonic current operator with an effective current operator. Inclusive electron scattering means that only the final momentum of the electron is measured. This means that the scattering cross-section involves a summation over all final states of the two nucleon system. Since the projectile and target are unpolarised, the cross-section can be written in terms of two response functions. The two response functions depend only on the momentum transfer $\vec{Q}$ and the energy transfer ω to the two nucleon system. The two response functions are called "longitudinal" and "transverse" response functions. They contain scattering states of the two nucleon system, the nucleonic current operator, and the two nucleon bound-state. I have derived the expressions for the response functions in a non-relativistic approximation.

The final states of the deuteron are all scattering states, since after inelastic scattering the deuteron is not in a bound state anymore. A direct calculation of the two response functions makes the explicit calculation of all scattering states of the two nucleon system necessary. This makes a direct calculation of the response functions a difficult task, especially for nuclei containing more than two electrons.

I therefore use a different method to calculate the response function in chapter 3. For this purpose I calculate the Stieltjes- and Lorentz-transforms of the response functions. This method makes use of the completeness relation of basis states. The Stieltjes-transform is calculated as the scalar product of the current operator applied to the two-nucleon bound state and another state $\left|\Phi_S\right\rangle$, which is the solution of an inhomogeneous Schrödinger-like equation involving negative energies. The Lorentz-transform is calculated as a scalar product of a state $\left|\Phi_L\right\rangle$ with itself. This state is also a solution of a similar inhomogeneous Schrödinger-like equation. In the case of the Lorentz-transform, there is an additional parameter σ_I that is involved. Theoretically, the back transformation process becomes easier as this parameter goes to zero. In practice, though, this leads to large numerical errors and hence an optimum value of σ_I needs to be chosen. The two inhomogeneous equations are easier to solve (compared to calculating scattering states of the nucleus) since they have no singularities. After this step, the problem is to back transform the integral transformations

to obtain the longitudinal and transverse response functions. It is important to note that the quality of the response function obtained from the back transformation strongly depends on the accuracy of its integral transforms. In this thesis, the Stieltjes transforms have been calculated with an accuracy of 6 significant digits. The Lorentz-transform was calculated with an accuracy of 5 significant digits.

The main difficulty with the back-transformation is that it is an ill-posed problem. This is because two very different response functions can have similar integral transformations. This makes our method of calculating the response functions very vulnerable to numerical errors. In general, the calculated Stieltjes or Lorentz-transforms need to be very accurate for the back transformation to yield an accurate response function. This is not always possible for systems with three or more nuclei. So far, either the Stieltjes-transform or the Lorentz-transform has been used to recover the response function. The idea in this thesis was to investigate the effect of using both integral transforms at the same time. For this purpose, a parameter for the relative weighting of both integral transforms in the back-transformation process was introduced.

In chapter 4 I first stated that the discretisation of the integral transforms leads to a singular system of linear equations. Back transformation involves solving this system of linear equations. The methods of Truncated Singular Value Decomposition (TSVD) and Tikhonov Regularization (TR) were used for this purpose. Both of these methods make use of the Singular Value Decompostion (SVD) of the integral transformation matrix. These methods have a parameter which is called the "regularisation parameter". A heuristic method called the "L-curve Method" exists in literature for the purpose of choosing an optimum value of the regularisation parameter in the TR method. It was found that this method was not useful for this particular case. Hence a scheme to determine the optimum values of these parameters was developed. The reasoning behind this scheme was to choose a regularisation parameter that gives minimum error and which is also grid independent.

The idea of using both integral transforms was first tested for the case of the Yamaguchi potential. Exact expressions for the response function were available in this case, which enabled us to analyse the effectiveness of using both integral transforms. Furthermore, a stability analysis of the back-transformation was performed and the effects of grid refinement and regularisation were studied. This analysis was carried out using only the Stieltjes-transform, only the Lorentz-transform, and both transforms. For the parameter σ_I the values 1.0 fm^{-1} and 0.1 fm^{-1} were used. It was found out that the value of 0.1 fm^{-1} is more suitable. It was also observed that response functions obtained using both integral transforms indeed have smaller errors.

It was observed from the test case, that response functions obtained using only the Stieltjes and only the Lorentz-transform have different characteristics in terms of non-physical behaviour. The response functions obtained from the Stieltjes transform have the tendency to become negative for higher values of the energy transfer ω. On the other hand, the response functions obtained from the Lorentz-transform have some oscillations present in the tail. The idea behind attempting to use both integral transforms for the purpose of the back

transform was that the information contained in them would complement each other and yield a response function free from their individual ill effects. This was indeed observed as the response function obtained using both integral transforms was non-negative. Unfortunately a small albeit noticeable deviation from the exact response function was observed. Nevertheless, using both integral transforms certainly provided some improvement over the approach of using a single integral transform.

Finally, in chapter 5 the back transformation techniques were applied to inclusive electron scattering using the Nijmegen-93 potential for nucleon-nucleon interaction. In this chapter, since exact expressions for the response functions were not available, a different scheme was developed to find the optimum value of the regularisation parameter. This scheme relied on a variation of the regularisation parameter. Since the TSVD method uses a discrete cutoff for the singular values, a slight variation of the regularisation parameter might or might not have an effect on the computed back transform. Unlike the TSVD method, the TR method uses a continuous function for the purpose of regularisation. This ensures that even a slight change in the value of the regularisation parameter has an effect on the calculated response function. Hence I decided to use only the TR method for the back-transformation. Both longitudinal and transverse response functions of the deuteron were calculated. The effects of grid refinement and the relative weight of the two integral transforms on the residual was studied. The Lorentz-weight (w_L) was chosen to account for the difference in the magnitudes of the Stieltjes and Lorentz-transforms of the longitudinal and transverse response functions.

The main aspect of this study was to investigate whether combined back transformations improve the results. I started with a test case where the exact response function was known apriori. Choosing the optimal values of the regularisation parameter was a straightforward task in this case. It was observed that the combined back-transformations did improve results in the test case. The experience from the test case was used for the more realistic case. Here the additional challenge was the fixing of the value of the regularisation parameter without apriori knowledge of the exact response function. Whereas we did not observe that combined transformations improved results in the longitudinal case, the behaviour for the transversal response function was better when both transformations were used. Nevertheless, the tail of the transversal response function did show some oscillations.

Outlook

An extension of the combined transforms method to 3-nucleon inclusive scattering has already been started. Besides, this procedure can be attempted with 4-nucleon systems using the Yakubovsky equations. For even more complex nuclei, other methods can be used to calculate the Stieltjes and Lorentz transforms. Further, it would be interesting to apply a statistical method for the back-transformation, that has been studied in [5], to the response functions. It has been applied in solid state physics. The nice feature of the method is the availability of error bars and the absence of any other parameters.

The results of this thesis are promising in the sense that the back transformations could be controlled without relying on special basis sets. This might open a path to use the transformation techniques for problems where the size of the structures is not very well known.

Appendices

A. Dirac Spinors and Gamma Matrices

The Dirac spinor is

$$\psi = u_{\vec{p},s} e^{-ipx} \tag{A.1}$$

, which is the plane wave solution of the free Dirac equation

$$(i\gamma^\mu \partial_\mu - m)\psi = 0. \tag{A.2}$$

The Dirac spinor can be written as

$$u_{\vec{p},s} = \sqrt{E_{\vec{p}} + m} \begin{bmatrix} \chi^s \\ \frac{\vec{\sigma}\cdot\vec{p}}{E_{\vec{p}}+m}\chi^s \end{bmatrix}. \tag{A.3}$$

For anti-particles we have

$$v_{\vec{p},s} = \sqrt{E_{\vec{p}} + m} \begin{bmatrix} \frac{\vec{\sigma}\cdot\vec{p}}{E_{\vec{p}}+m}\chi^s \\ \chi^s \end{bmatrix}. \tag{A.4}$$

Here,

$$\begin{aligned} \chi^1 &= \begin{bmatrix} 0 \\ 1 \end{bmatrix} \\ \chi^2 &= \begin{bmatrix} 1 \\ 0 \end{bmatrix}. \end{aligned} \tag{A.5}$$

The completeness relations for the four-spinors u and v are

$$\begin{aligned} \sum_{s=1,2} &= u_p^{(s)} \bar{u}_p^{(s)} = \not{p} + m \\ \sum_{s=1,2} &= v_p^{(s)} \bar{v}_p^{(s)} = \not{p} - m \end{aligned} \tag{A.6}$$

where,

$$\begin{aligned} \not{p} &= \gamma^\mu p_\mu \\ \bar{u} &= u^\dagger \gamma^0. \end{aligned} \tag{A.7}$$

I have made use of the Gamma-matrices in the Dirac representation, they are

$$\gamma_0 = \begin{bmatrix} 0 & 1 \\ 1 & 0 \end{bmatrix}$$
$$\gamma_k = \begin{bmatrix} 0 & \sigma_k \\ -\sigma_k & 0 \end{bmatrix}. \tag{A.8}$$

Finally

$$\sigma_{\mu\nu} = \frac{i}{2}[\gamma_\mu, \gamma_\nu]. \tag{A.9}$$

B. Clebsch-Gordan Coefficients, Tensor Operators and Partial Wave Relations

In this appendix I will list all the partial wave relations I used frequently. In the following equations, the λ sub- or super-script denotes the spherical component of a vector.

$$\vec{q}_\lambda = q\sqrt{\frac{4\pi}{3}}Y_{1\lambda}(\hat{q}) \tag{B.1}$$

In equations (B.2) and (B.3), $\{\cdot,\cdot\}^{kq}$ represents a coupling of tensor operators to the q^{th} component of a tensor operator of order k.

$$\vec{a}\cdot\vec{b} = -\sqrt{3}\{a,b\}^{00} \tag{B.2}$$

$$(\vec{a}\times\vec{b})_\lambda = -\sqrt{2}i\{a,b\}^{1\lambda} \tag{B.3}$$

In equation (B.4) $\hat{e}_z$ is the unit vector in the Z direction.

$$Y_{lm}(\hat{e}_z) = \sqrt{\frac{\hat{l}}{4\pi}}\delta_{m0} \tag{B.4}$$

$$\int_0^{2\pi} d\varphi Y_{lm}(\theta,\varphi)Y_{l',m'}(\theta',\varphi) = 2\pi Y_{lm}(\theta,0)Y_{l'm'}(\theta',0)\delta_{mm'} \tag{B.5}$$

Clebsch-Gordan coefficients.

$$\left\langle jm_j j'm'_j \middle| (jj')Jm_J \right\rangle = (jj'J, m_j m'_j m_J) \tag{B.6}$$

T^q_k represents the q^{th} component of a k^{th} order tensor operator. Tensor operators T^q_k and $\tilde{T}^{q'}_{k'}$ can be coupled to an operator $\mathbb{T}^Q_K$.

$$\mathbb{T}^Q_K = \sum_{qq'}(kk'K, qq'Q)T^q_k\tilde{T}^{q'}_{k'} \tag{B.7}$$

Now I state in equation (B.8) the equation for the Wigner-Eckart theorem. $\langle j' \| T_k \| j \rangle$ is the reduced matrix element and it is independent of m and m'.

$$\langle j'm' | T_k^q | jm \rangle = (jkj', mqm') \langle j' \| T_k \| j \rangle \tag{B.8}$$

The following equation is a way to calculate reduced matrix elements of coupled angular momentum states and coupled tensor operators. The two reduced matrix elements can be calculated using the Wigner-Eckart theorem.

$$\langle (j_1' j_2') j' \| \{T_{k_1}, \tilde{T}_{k_2}\}^k \| (j_1 j_2) j \rangle = \sqrt{\hat{j}_1' \hat{j}_2' \hat{j} \hat{k}} \begin{Bmatrix} j_1' & j_1 & k_1 \\ j_2' & j_2 & k_2 \\ J' & J & K \end{Bmatrix} \langle j_1' \| T_{k_1} \| j_1 \rangle \langle j_2' \| \tilde{T}_{k_2} \| j_2 \rangle \tag{B.9}$$

Overlaps between different basis states:

$$\langle \vec{p} | p' l m \rangle = Y_{lm}(\hat{p}) \frac{\delta(p - p')}{p \cdot p'} \tag{B.10}$$

l is the angular momentum quantum number and m is the Z component

$$\langle p l m_l s m_s | p' (l' s') j' m_j' \rangle = \frac{\delta(p' - p)}{p \cdot p'} \delta_{ll'} \delta_{ss'} (l' s' j', m_l m_s m_j'). \tag{B.11}$$

Bibliography

[1] V D Efros. *Soviet Journal of Nuclear Physics*, 41:949, 1985.

[2] V D Efros, W Leidemann, G Orlandini, and N Barnea. The lorentz integral transform (LIT) method and its applications to perturbation-induced reactions. *Journal of Physics G: Nuclear and Particle Physics*, 34(12):R459, 2007.

[3] V.D. Efros, W. Leidemann, and G. Orlandini. Electron scattering response functions from their stieltjes transforms. *Few-Body Systems*, 14(4):151–170, 1993.

[4] L D Faddeev. Scattering theory for a three-particle system. *Soviet Physics JETP*, 12(5):1014 – 1019, 1961.

[5] K Ghanem. Stochastic mode sampling (SMS) – An efficient approach to the analytic continuation problem. Unpublished Thesis, October 2013.

[6] J. Golak, H. Kamada, H. Witała, W. Glöckle, and S. Ishikawa. Electron induced *pd* and *ppn* breakup of ^{3}He with full inclusion of final-state interactions. *Phys. Rev. C*, 51(4):1638–1647, Apr 1995.

[7] J. Golak, R. Skibiński, H. Witała, W. Glöckle, A. Nogga, and H. Kamada. Electron and photon scattering on three-nucleon bound states. *Physics Reports*, 415(2–3):89 – 205, 2005.

[8] P C Hansen. Analysis of discrete ill-posed problems by means of the L-curve. *SIAM Review*, 34:561–580, 1992.

[9] Per Christian Hansen. Truncated singular value decomposition solutions to discrete ill-posed problems with ill-determined numerical rank. *SIAM J. Sci. Stat. Comput.*, 11(3):503–518, May 1990.

[10] S. Ishikawa, H. Kamada, W. Glöckle, J. Golak, and H. Witała. Response functions of three-nucleon systems. *Physics Letters B*, 339(4):293 – 296, 1994.

[11] F. Mandl and G. Shaw. *Quantum Field Theory*. A Wiley-Interscience publication. John Wiley & Sons, 2010.

[12] S. Martinelli, H. Kamada, G. Orlandini, and W. Glöckle. Longitudinal response functions of ^{3}He and ^{3}H by lorentz kernel transformations. *Phys. Rev. C*, 52:1778–1782, Oct 1995.

[13] A Nogga. Inklusive electronenstreuung an ^{3}He und ^{3}H. Unpublished Thesis, October 1995.

[14] J. J. Sakurai. *Modern Quantum Mechanics (Revised Edition)*. Addison Wesley, revised edition, September 1993.

[15] V. G. J. Stoks, R. A. M. Klomp, C. P. F. Terheggen, and J. J. de Swart. Construction of high-quality *NN* potential models. *Phys. Rev. C*, 49:2950–2962, Jun 1994.

[16] A N Tikhonov. On the stability of inverse problems. *Doklady Akademii Nauk SSSR*, 39(5):195–198, 1943.

[17] Lloyd N. Trefethen and David Bau III. *Numerical Linear Algebra*. SIAM: Society for Industrial and Applied Mathematics, 1997.

[18] O Yakubowsky. *Soviet Journal of Nuclear Physics*, 5:937, 1967.

[19] Yoshio Yamaguchi. Two-nucleon problem when the potential is nonlocal but separable. I. *Phys. Rev.*, 95:1628–1634, Sep 1954.